
The Influence of Winter Cloud on Summer Sea Ice in the Arctic, 1982-2013

Author:

Aaron D. Letterly

Advisor:

Dr. Steven A. Ackerman

A thesis submitted in partial fulfillment of
the requirements for the degree of

Master of Science

(Atmospheric and Oceanic Sciences)

at the

UNIVERSITY OF WISCONSIN-MADISON

May 2015

Thesis Declaration and Approval

I, Aaron D. Letterly, declare that this thesis titled, ‘The Influence of Winter Cloud on Summer Sea Ice in the Arctic, 1982-2013’ and the work presented in it are my own.

Aaron D. Letterly
Author

Signature

Date

I hereby approve and recommend for acceptance this work in partial fulfillment of the requirements for the degree of Master of Science:

Steven A. Ackerman
Director, CIMSS

Signature

Date

Jeffrey R. Key
Faculty Member

Signature

Date

Tristan L’Ecuyer
Faculty Member

Signature

Date

Abstract

Recent, inter-annual variability in Arctic sea ice area suggests that the pole's ice cover is vulnerable to drastic change over yearly timescales. Large variations in late summer ice concentration occur in marginal ice areas such as the Beaufort and Chukchi Seas, despite the hemispheric trend of decreasing sea ice. Ice cover in these areas is thin enough that its extent and concentration can fluctuate significantly between years. Clouds over these regions represent one of the most fundamental, but also complex, contributors to the local surface radiation budget. In this study, the strength and significance of winter clouds' role in summer ice concentration is examined statistically and physically. Here, we determine that winter clouds contributed to the 2012 summer sea ice minimum, and observe through model reanalysis and satellite remote sensing two separate regimes of cloud forcing anomaly from 1982-1997 and 1998-2013. A simple ice growth model estimated that from 1998-2013, anomalous cloud forcing contributed downwelling energy with the potential to decrease ice thicknesses by 1.45 m. The opposite effect, or an increase in summer ice thickness, was observed for the early period with negative cloud forcing anomalies. Large-scale atmospheric and ocean dynamics in the Beaufort and Chukchi Seas further amplify these regions' effect on hemispheric ice totals by advecting ice concentration anomalies elsewhere in the Arctic. Though many factors impose significant forcing on sea ice growth and loss, the substantial variance in cloud cover over the winter months contributes significantly to inter-annual sea ice variability.

Contents

Abstract.....	i
1. Introduction.....	1
2. Data and Methods	8
3. Winter 2012 Cloud Amount.....	155
4. Winter 1984 Cloud Amount.....	266
5. Climatological Relationship between Cloud Forcing and Sea Ice Concentration, 1982-2013.	30
6. Influences of Wintertime Cloud forcing on Summertime Sea Ice Concentration	399
7. Conclusions.....	46
8. Future Work	50
Acknowledgements.....	522
References.....	533

List of Figures

Figure 1. Equal-Area Arctic Map with regions of interest..	5
Figure 2. 500 hPa average geopotential height anomalies, January-March 2012..	16
Figure 3. ERA-Interim longwave cloud forcing, 2011-2012 winter.	18
Figure 4. ERA-Interim surface cumulative longwave cloud forcing anomalies, 2012..	19
Figure 5. MODIS, MERRA cloud cover anomalies and cloud forcing anomalies.....	21
Figure 6. MERRA ice thickness change and SSMI ice concentrations	23
Figure 7. MERRA Ice thickness distribution anomalies	24
Figure 8. MERRA cumulative cloud forcing anomalies.	27
Figure 9. ERA cumulative cloud forcing anomaly	28
Figure 10. MERRA ice thickness change and SSMI concentrations.....	289
Figure 11. MERRA correlation map, clouds forcing ice.	342
Figure 12. ERA correlation map, clouds forcing ice.	34
Figure 13. MERRA correlation map, ice forcing cloud.....	345
Figure 14. MERRA correlation map series, ice forcing cloud..	347
Figure 15. MERRA cloud forcing and SSMI ice concentration timeseries	38
Figure 16. APP-x ice thickness climatology.....	39
Figure 17. Linear regression of Beaufort Sea cloud forcing on sea ice	42
Figure 18. Time series of clouds, ice, and climate indices	44
Figure 19. MERRA Beaufort Sea correlation map	45

Abbreviations

AO	Arctic Oscillation
APP-x	AVHRR Polar Pathfinder- Extended
C	Celsius
CALIOP	Cloud-Aerosol Lidar with Orthogonal Polarization
CALIPSO	Cloud Aerosol Lidar and Infrared Pathfinder Satellite Observation
DMSP	Defensive Meteorological Satellite Program
EASE	Equal Area Scalable Earth
ECMWF	European Centre for Medium-range Weather Forecasting
ENSO	El Niño Southern Oscillation
ERA	ECMWF Reanalysis
hPa	hectoPascals
K	Kelvin
km	kilometer
m	meter
MERRA	Modern Era Retrospective Analysis for Research and Applications

MODAPS	MODIS Adaptive Processing System
MODIS	Moderate Resolution Imaging Spectroradiometer
MS2GT	MODIS Swath 2(to) Grid Transfer
<i>n</i>	Degrees of Freedom
NASA	National Aeronautics and Space Administration
NCDC	National Climatic Data Center
NOAA	National Oceanic and Atmospheric Administration
NSIDC	National Snow and Ice Data Center
PDO	Pacific Decadal Oscillation
PNA	Pacific North American Mode
<i>r</i>	Pearson's Correlation Coefficient
SSM/I/S	Special Sensor Microwave Imager/Sounder

1. Introduction

Over the last decade, the Arctic has suffered a significant decline in sea ice extent. The decreasing ice area corresponds to a warming of the Arctic at more than twice the global average, known as Arctic amplification. Though Arctic amplification is anticipated to cause warming through the year 2100 (Holland and Bitz 2003, Zhang and Walsh 2006, Overland and Wang 2013), inter-annual variation in Arctic sea ice extent remains unpredictable. The variables affecting sea ice growth include, but are not limited to, large-scale atmospheric circulation, local meteorology, and surface fluxes. Cloud cover also affects sea ice, but the forcing depends on both the phase and thickness of clouds. The distinct Arctic seasons result in variations of the magnitude and sign of the forcing.

Cloud forcing is defined as the difference in radiative components of an energy budget between clear-sky and all-sky conditions, implying that the presence (or absence) of clouds may have an appreciable radiative effect on the surface. Though the net cooling or warming effects of clouds over the Arctic surface cycles semi-annually, their contribution to the surface energy budget of the Arctic (Curry *et al* 1996, Intrieri *et al* 2002, Liu *et al* 2008, Tjernström *et al* 2008) is substantial. The lack of sunlight during the Arctic winter leaves the absorption and emission of the earth's longwave radiation by clouds as the primary radiative forcing. Serving to couple the surface and free troposphere, clouds play a crucial role in sea ice growth and loss. In this study, longwave anomalies caused by cloud forcing are of particular interest, and will be explored both statistically and climatologically. Understanding the relationship between wintertime clouds and summertime ice concentration anomalies will aid in determining whether clouds play a

significant role in abrupt year-to-year ice concentration changes, the long-term hemispheric sea ice decline, or both.

Arctic sea ice extent is forced by a range of feedback mechanisms, with ice-albedo and cloud feedbacks contributing significantly towards sea ice growth and melt (Serreze and Francis 2006, Curry *et al* 1996). Over recent decades, a record of seasonal changes in Arctic cloud amount affecting surface energy fluxes has been provided by many satellite-derived products (Liu *et al* 2007, 2008, 2009, Wang and Key 2003, 2005, Schweiger 2004). While local processes affecting the energy budget on inter-annual timescales contribute readily to yearly changes in ice extent, large-scale atmospheric variability has also been shown to contribute to the sea ice decline, particularly changes in such modes of circulation as the Northern Annular Mode (Deser and Teng 2008, Ogi and Rigor 2013) and the Arctic Dipole Anomaly pattern (Overland *et al* 2012, Wang *et al* 2009).

The ability for sea ice changes to affect changes in cloud cover is well-documented (Vavrus *et al* 2009, 2011, Schweiger *et al* 2008a, Cuzzone and Vavrus, 2011, Kay and Gettelman 2009, Palm *et al* 2010, Liu *et al* 2012a), but the changes clouds induce on sea ice are less studied. Since the surface net radiative effect of Arctic clouds vary by season, their yearly impact on a warming Arctic can be nebulous. Pithan and Mauritsen (2013) polled a spread of climate models to determine the effect of clouds on surface temperatures. Their results showed that climate models gave different answers regarding the net warming or cooling effect of clouds on the Arctic surface. It was determined that cloud cover most strongly contributed via increasing downwelling longwave radiation, thereby raising surface temperatures and favoring Arctic amplification. Current scientific literature investigating Arctic surface-cloud interactions

supports this result; increased downwelling longwave radiation caused by springtime cloud cover corresponds to years with negative sea ice anomalies (Graversen et al 2011, Kapsch et al 2013).

Research on the effects of downwelling shortwave anomalies on sea ice has contrasting results. Nussbaumer and Pinker (2012) found that ice areas receiving the largest amounts of downwelling shortwave radiation from January through June do not correspond to negative sea ice concentration anomalies. Opposite to the findings of Nussbaumer and Pinker, Kay *et al* (2008) used reanalyses (not observations) to determine that decreases in cloud cover increased downwelling shortwave radiation at the surface and contributed to the 2007 ice extent minimum, citing 2.4 K of warming to the ocean by cloud and radiation anomalies alone. Schweiger *et al* (2008b) however, found that negative cloud anomaly resulting in increased downwelling shortwave flux over the summer months had no appreciable contribution to the sea ice extent minimum. Kauker *et al* (2009) discussed the minor impacts of clouds reductions in summer on ice extent, but related the 2007 minimum to be chiefly caused by wind conditions in May and June, surface temperature in September, and ice thickness in March. Perovich *et al* (2008) assigned the primary cause of enhanced ice loss in the Beaufort Sea during the summer of 2007 to be enhanced heating of the upper ocean, though cloud effects on this heating were not explicitly mentioned.

Many of these studies are devoted to the effects of clouds on spring or summer radiative budget; both seasons represent regimes in which downwelling shortwave is one of the strongest contributors to the surface energy budget. Clouds effectively warm the Arctic surface except in the summer (Intrieri et al 2002, Schweiger and Key 1994, Stone 1997). Stone et al. (2005) showed that during February at Barrow, Alaska, a 5% increase in cloud cover produced an increase in surface temperature of 1.4°C on average over a 33-year period. These findings by

Stone et al. (2005) illustrate the contribution of changing wintertime clouds on a climatological basis, rather than a seasonal one. Increased cloud cover in winter warms the surface with emitted longwave radiation. Stone et al (2005) refers to the heating by wintertime clouds as "ripening" the surface snow cover for increased summer melt by downwelling solar radiation in May and June. This preconditioning of the winter surface may also be applied to sea ice, and is increased during winters that experience warm air incursions from mid-latitudes. From a multi-year perspective, enhanced cloud cover during winter, followed by summers of average downwelling shortwave, could result in a feedback of weaker refreezing and ultimately, thinner and less ice.

By this convention, an enhancement of downwelling longwave energy by clouds during winter inhibits surface cooling and stifles sea ice growth. The influence of wintertime cloud cover and surface radiation anomalies has been explored at length (Curry et al. 1996), but their relationship with summertime sea ice concentration has not been explicitly addressed until their and was examined by Liu and Key (2014). The notion of atmospheric "memory," particularly over the Arctic, is explored in a summer ice and autumn weather relationship in Francis et al. (2009). This system memory is further explored by Liu and Key's (2014) use of multiple climate reanalyses to determine that anomalously low cloud cover in the winter of 2013 contributed to the summertime sea ice area rebound from the record low of 2012. They verified their reanalyses with remotely sensed products from the Moderate Resolution Imaging Spectroradiometer (MODIS), the Cloud-Aerosol Lidar with Orthogonal Polarization (CALIOP) , and Cryosat-2, as well as aircraft data. Their analysis confirmed that winter cloud cover anomalies can significantly affect year-to-year variations in summer sea ice cover.



Figure 1. Equal-Area projection map of the Arctic. The region of interest spans from the Beaufort Sea to the Eastern Siberian Sea, spanning the Bering and Chukchi Seas.

Much of the analysis by Liu and Key (2014) as well as many of the other studies referenced here investigate how changes in the energy budget affected changes in sea ice over

the western Arctic. This region encompasses a range of sea ice thicknesses and ages, from thin seasonal ice near the Bering Strait inflow to the multi-year ice off the northern coast of Greenland several meters thick. The Mackenzie River is the only large freshwater inflow to this region. The Beaufort Sea is situated due north from the Aleutian Low pressure zone, an atmospheric mode of circulation in the Gulf of Alaska. Each year, cyclones tracking northward over the Alaskan mainland or through the Bering Strait bring warm air and high winds to this region, further impacting ice cover and the general circulation of the region itself (Rodionov *et al* 2007). This region of the Arctic is also influenced by the Beaufort Gyre, a semi-permanent high-pressure circulation. The gyre rotates clockwise, eventually churning water and ice off Canadian and Alaskan shores westward over Siberia and then again northward where advected ice converges with the Central Arctic core of thick, multi-year pack ice. This circulation also feeds into the Transpolar Drift stream, which transports ice from the Laptev sea across the North Pole and out through the Fram Strait. The complex ice, ocean, and atmospheric dynamics, this zone may be a reason it experiences such a large range in cloud coverage and ice concentration from season to season.

This study extends the work of Liu and Key (2014) by examining the role of wintertime cloud anomalies on summertime sea ice concentration. Additionally, the winter preceding the 2012 sea ice minimum is used as a case study examining the inter-annual effects of cloud forcing on rapid sea ice change. Arctic clouds are then analyzed in a climatological context by determining long-term radiative contributions and trends over the satellite record. Obtained results from climate reanalysis output are supported by passive remote sensing products where possible. Special attention is given to the ten-year period from 1997-2012 in which cloud forcing anomaly over the Beaufort Sea was consistently positive, verifiable by current-generation

satellite products, and corresponded to multiple years of record-setting sea ice area minimums. Though large-scale atmospheric heat transport and ice dynamics undoubtedly made some contribution to the significant decrease in sea ice extent over this time period, this study does not attempt to address these factors. Instead, it focuses on the increases and decreases in winter cloud cover that, year after year, precondition the Beaufort Sea for rapid changes in sea ice area.

2. Data and Methods

Longwave radiation from two model reanalyses was analyzed over the thirty-two year satellite record to determine the mean and anomalous behavior of clouds in the Beaufort Sea. Based on the climatological mean for a given month, individual monthly anomalies were assessed. Their radiative contribution to the surface was tabulated, and in some cases, used to calculate the changes in ice thickness based on this anomaly. Negative winter cloud cover anomalies in 1984 and positive winter cloud cover anomalies 2012 were studied to determine the effects of winter cloud forcing on end-of-summer ice concentration. While Arctic amplification affects feedbacks over all seasons when the sun is present, this study specifically looks at sea ice concentration anomalies in September, when ice extent and thickness is at a yearly minimum after months of summer insolation. Lagged correlations between the total winter seasonal cloud forcing anomaly and September ice concentration anomaly were generated in an effort to provide a summary of the relationship between clouds and sea ice in marginal ice areas of the Arctic. The anomalies and effects of cloud forcing for specific case studies are supported by remotely-sensed cloud cover, ice thickness, and ice motion.

A daily sea ice concentration (defined as the percentage of sea ice in a single pixel of a gridded spatial domain) product based on the NASA (National Aeronautics and Space Administration) Team algorithm (Cavalieri *et al* 1996, Maslank and Stroeve 1999), with brightness temperature data from the Defense Meteorological Satellite Program (DMSP) –F8, -F11 and –F13 Special Sensor Microwave/Imager (SSM/I), and the DMSP-F17 Special Sensor Microwave Imager/Sounder (SSMIS), was obtained from NSIDC. The product was gridded to 25 x 25 km resolution.

Also employed in this study is the NASA Modern-era Retrospective Analysis for Research and Applications (MERRA) reanalysis (Rienecker *et al* 2011). MERRA covers the modern era of remotely sensed data, from 1979 through the present at 2/3-degree longitude by 1/2-degree latitude. Here, output is analyzed on monthly timescales, though daily and hourly data is available.

The European Centre for Medium-Range Weather Forecasts (ECMWF) ERA-Interim Reanalysis ('ERA-Interim') is also used, primarily as a preliminary assessment of atmospheric pressure and cloud conditions. ERA-Interim is the latest ECMWF global atmospheric reanalysis (Dee *et al* 2011). The ERA-Interim project replaces the previous atmospheric reanalysis ERA-40 and covers the period of 1979 through the present. Reanalysis variables of interest here include cloud cover (total, low-, mid-, and high-level), surface radiation, and geopotential height. Both reanalyses yield similar results for this study, and products from each reanalysis are often presented together, with differences noted where significant.

Both MERRA and APP-x products were transformed using the MODIS Swath to Grid Transfer (MS2GT) tool so that pixel-by-pixel analyses could be performed. ERA-Interim data at T255 spectral (~80 km) resolution was remapped to fit with the MERRA data at finer resolutions (0.66° longitude by 0.5° latitude). Other datasets employed in this study include sea ice thickness estimates based on monthly averages of the Polar Pathfinder (APP-x) daily product (Wang *et al.*, 2015), which was remapped to MERRA resolution (from the native 5km resolution), as well as sea ice motion vectors from the Polar Pathfinder daily, 25 km EASE-Grid product (Fowler *et al* 2013).

Arctic cloud cover is determined primarily with data from MODIS onboard the NASA Terra and Aqua satellites. MODIS measures radiances at 36 wavelengths, including infrared and

solar bands, with spatial resolution of 250m-1km. This robust set of measurements provides the potential for improving cloud detection in the Arctic (Ackerman *et al* 1998, 2008, Frey *et al* 2008). While improvements to MODIS cloud detection have been made (Liu *et al* 2004, Frey *et al* 2008), there are still larger errors in nighttime Arctic cloud detection than for most other regions on Earth (Holz *et al* 2008). MODIS data were obtained from the Atmosphere Archive and distribution System of the NASA Goddard Space Flight Center. Terra MODIS data for the period 2002-2013 are used here.

Over the Canada basin, MODIS monthly cloud cover anomalies were in close agreement with calculated MERRA cloud forcing for the same time period. Liu and Key (2014) established that the MERRA reanalysis closely resembled both spatial patterns and magnitudes of satellite cloud products from the Cloud-Aerosol Lidar and Infrared Pathfinder Satellite Observation (CALIPSO) and MODIS. Similarities between model and satellite data encouraged further analysis using point-by-point correlations between MERRA cloud forcing and the NASA sea ice concentration product.

Since this study focuses on wintertime cloud cover on summer sea ice concentration, cloud forcing values were averaged over the months of October through March and ice concentration was determined for September, widely regarded as the end of the summer melting season. Cloud "forcing," or "radiative effect," refers to the difference in the net radiation flux between clear sky and cloudy conditions. Anomalies in cloud forcing are here defined as the departure from the 1982-2013 mean radiative effect that clouds impose on upwelling and downwelling longwave and shortwave radiation. Defined mathematically, cloud forcing is the integrated partial derivative of the radiative flux with respect to the cloud fraction and takes the forms

$$CS_S = \int_0^{A_c} \frac{\partial S_S}{\partial a} da = S_S(A_c) - S_S(0) \quad (1)$$

$$CF_S = \int_0^{A_c} \frac{\partial F_S}{\partial a} da = F_S(A_c) - F_S(0) \quad (2)$$

$$CNET_S = CS_S + CF_S \quad (3)$$

where CS, CF, and CNET are the shortwave, longwave, and net cloud forcing at the surface (subscript s), A_c is the total cloud amount, S_S and F_S are the net shortwave and longwave fluxes at the surface, and a is the cloud fraction. To represent the total seasonal cloud forcing anomaly, the monthly anomaly fields were summed over the six winter months into a single value, hereafter referred to as the "cumulative cloud forcing." This number was then used to determine the radiative effect of anomalous cloud forcing on ice growth over a single season. Since downwelling shortwave is minimal over the winter months, CS_S in all further equations is considered to be zero which isolates the effects of longwave radiative anomalies on ice concentration.

The approximate contributions of the cloud forcing anomaly to changes in ice thickness by cloud forcing anomaly can be calculated. Negative surface cloud radiative forcing anomalies favor sea ice growth, while positive anomalies inhibit ice formation. Thorndike (1992) presented a simple method to relate a change in ice thickness to surface net radiation:

$$\Delta h = \frac{t}{\rho L} [F_S + S_S + F_W] \quad (4)$$

where t is the length of the time period, ρ is the density of sea ice (917 kg m^{-3}), L is the latent heat of fusion for sea ice (333.4 kJ kg^{-1}), F_S is the surface net longwave radiation, S_S is the

surface net shortwave radiation, and F_w is the conductive heat flux at the ice-ocean interface.. This equation bears similarities to Eisenman *et al* (2007). Turbulent surface fluxes such as sensible and latent heat as well as the conductive flux are neglected in this model, as they are much smaller than the radiative fluxes. To determine only the effects of cloud forcing on ice growth this equation can be rewritten as

$$\Delta h = \frac{t}{\rho L} [\text{CNET}_S - F_{\text{net}}(0)] \quad (5)$$

where $F_{\text{net}}(0)$ is the surface net radiation for clear sky and CNET_S is the surface net cloud radiative forcing. Ignoring turbulent and conductive heat fluxes introduces some error. For example, the conductive heat flux is likely to decrease with increased ice thickness, so that ice growth will be smaller for thicker or colder (more degrees below 0°C) sea ice with the same cloud radiative forcing. Surface emissivity, albedo, and the conductive heat flux are functions of snow depth, and uncertainty in the snow depth would also lead to some error in sea ice growth estimates. Using the above method, 1 W m⁻² of negative monthly net cloud radiative forcing anomaly would theoretically grow 0.85 cm of sea ice. This equation assumes a surface temperature of ice near 0° C. Less change in the ice column height would occur if the ice first needed to be “heated” to 0°C before melting. Sea ice growth resulting from the cumulative October-March cloud forcing anomaly can be calculated from the MERRA cloud radiative forcing.

A battery of simple statistical procedures that compare the multiple reanalyses and variables of interest referenced in this study are performed. To determine the degree of dependence between two variables, a simple lagged Pearson correlation coefficient (r) is computed. The length of this lag time ranges from 11 months (October-September) to 6 months

(March-September), giving a mean lag of 9 months when cumulative monthly winter values are used. Further insight regarding the relationship between two variables is gained by testing for the significance of the correlation coefficient between variables tested. The significance of the relationship is expressed in probability levels (i.e., significant at the 50 per cent confidence interval), which tell how unlikely a given correlation coefficient will occur given no relationship between any two variables. This significance test assumes a sample relationship from a population and determines whether the relationship is likely to be observed based on the size of the population.

In this study, the statistical null hypothesis is that there is no relationship between winter cloud forcing and summer ice concentration ($r=0.0$). When the magnitude of the correlation coefficient is far enough from this assumption, the resulting statistic is considered significant and the null hypothesis of no relationship between clouds and ice may be rejected. The difference in magnitudes between the null hypothesis and the sample relationship (t) for significance at some confidence interval is determined by the formula

$$t = r \sqrt{\frac{n - 2}{1 - r^2}} \quad (6)$$

where n is the degree of freedom, which is based on the sample population. When the computed value of t is higher than the corresponding distribution critical value, the null hypothesis is rejected. It can therefore be interpreted that when the strength of correlation and related variance (r^2) between two variables is low, the computed t -values will be lower than the critical t -value, and then null hypothesis cannot be rejected. In this way, we may determine where the

relationship between winter cloud forcing and summer sea ice concentration is statistically significant, rather than due to sampling error. This study assigns statistical significance when the null hypothesis is rejected at the 95 per cent (.95) confidence level.

3. Winter 2012 Cloud Amount

September 2012 marked the minimum Arctic sea ice extent over the satellite record. A report by the National Snow and Ice Data Center noted that a storm system in August over the Central Arctic caused the thin seasonal ice to melt and break apart. Though the central Arctic Ocean is normally covered in ice and surrounded by thinner first-year ice, this storm was cited as a main reason for the sea ice minimum. In this section we posit that positive cloud anomalies during winter over marginal ice areas, notably from the Beaufort Sea west to the Chukchi Sea, led to a weak winter refreezing and ultimately served to precondition the exposed Central Arctic for a large melting event. Liu and Key (2014) conducted a similar study for 2013, but focused on negative cloud anomalies over winter. Their work demonstrated spatial and physical connections between significantly below normal winter cloud cover and increased ice thicknesses contributing to a large rebound in September ice area extent relative to the 2012 minimum. This section focuses on the causes and effects of increased winter cloud cover in 2012 seen by reanalysis. Reanalysis are based on very simple cloud parameterizations, and, for comparison, passive remote sensing products are used to support the spatial patterns and magnitudes of cloud cover anomaly over various regions.

The winter preceding the sea ice minimum in September 2012 saw significant cloud cover anomalies that were indicative of increased downwelling longwave radiation. The cloud cover anomaly pattern corresponds to a negative geopotential height anomaly over a similar region (Figure 2). This anomalously low pressure system may be the cause of the positive cloud amount anomaly. Negative wintertime height anomalies generally result in greater wintertime cloud cover (Liu *et al* 2007, 2008). This geopotential anomaly is confirmed in the ERA-Interim

500 hPa Geopotential Height Anomalies (Jan-Mar 2012)

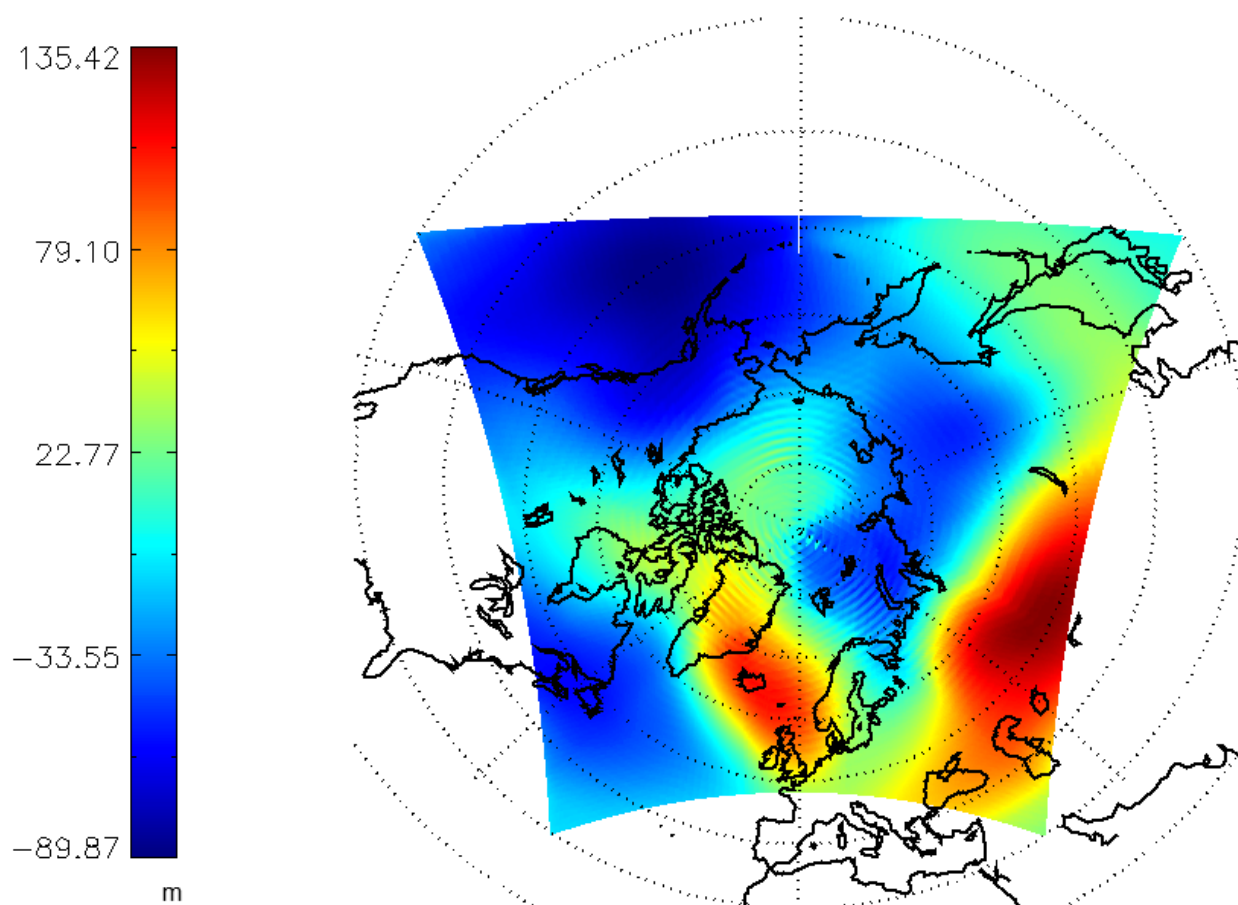


Figure 2. The 500 hPa average geopotential height anomalies (unit: m) from ERA for January-March 2012. The anomalies are calculated relative to the 1982-2013 mean for the respective months.

reanalysis, where anomalously low geopotential heights (in hectopascals, hPa) over the Alaskan and Eastern Siberian Arctic correspond to the positive anomalies in cloud amount. Regions of low pressure indicate a stronger upward vertical motion, indicating increased convection and greater cloud cover while anomalies persist. During the first half of the winter (October-December), ERA geopotential height anomalies show neutral to positive values over the Beaufort and Chukchi Seas, implying sinking air and generally fewer clouds.

ERA-Interim longwave cloud forcing shows a development of cloud cover anomalies over the 2011-2012 winter that corresponds spatially with low geopotential heights, cloud cover from other reanalyses, and cloud amount fields from remote sensing. Over a six-month period, marginal ice zones in the Beaufort, Chukchi, and East Siberian Seas experienced longwave cloud forcing anomalies that were anomalously positive, i.e., a greater warming effect. Increased cloud amount in these regions throughout the winter was an important factor in keeping sea ice from attaining typical thicknesses, which, as explained below, ultimately contributed to the sea ice minimum in September.

October 2011 shows a region of elevated downwelling longwave cloud forcing centered over Alaska and west Siberia, whereas much of the central Arctic Ocean has very little cloud forcing. Values of longwave cloud forcing near zero indicate no difference between a "clear sky" and "all sky" (which includes clouds) in the model. In October, the majority of the Barents and Kara Seas show no longwave cloud forcing, meaning they were nearly cloud-free. This pattern of enhanced cloud forcing persists through November, though the larger values over Alaska and the Siberian Arctic become more cut off from the weaker cloud forcing in the Pacific and continents. During December, the bull's eye of elevated cloud forcing diminishes in both spatial area and magnitude. The Barents and Kara Seas experience a resurgence of negligible cloud cover during

this time. From January-March of 2012, the longwave cloud forcing over the Beaufort Sea was consistently 60W/m^2 , peaking in February. By March 2012, the Arctic from the Canadian Archipelago to the Eastern Siberian Sea had experienced six months of positive cloud forcing anomalies, preconditioning the ice for an unprecedented melt event in the following spring and summer.

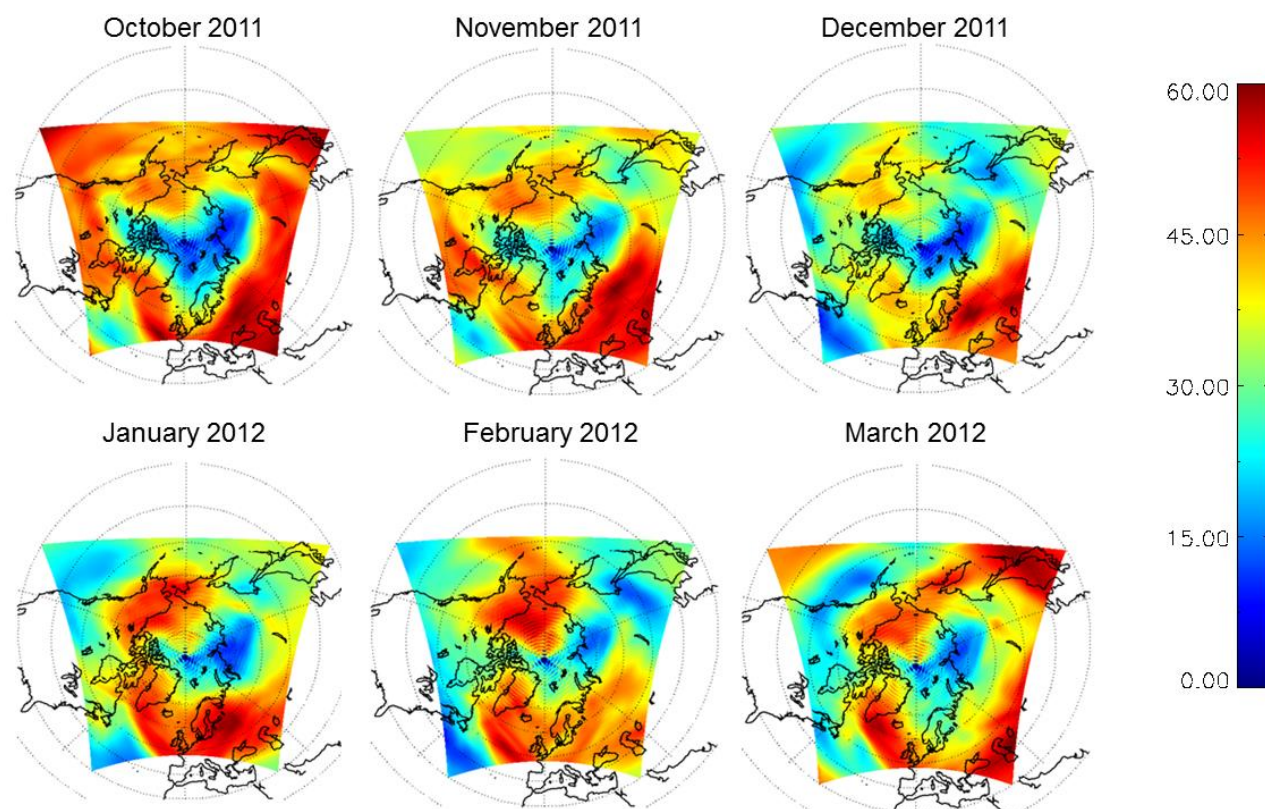


Figure 3. Longwave cloud forcing fields for the 2011-2012 winter calculated from the ERA-Interim Reanalysis. Values of zero represent a transparent cloud layer or the clear sky.

The cumulative cloud forcing anomaly over the 2011-2012 winter for ERA-Interim reanalysis verifies that the elevated cloud forcing over the Beaufort Sea western Canadian Arctic was anomalously positive. A region of negative cumulative cloud forcing anomalies extends over the Chukchi and East Siberian Sea, but the majority of these negative anomalies occur over

land or too far south to be effective in modifying sea ice concentration and thickness. The enhanced cloud forcing extending northward from the Alaskan coast lies over an area of the Beaufort Sea that experienced dramatic sea ice loss by late summer, lending credence to anomalous winter clouds' capability to impact ice area at the end of a melting season.

While the two reanalyses used in this study (MERRA and ERA) typically are in agreement, the differences in observations and data processing cause some differences to arise (Rienecker *et al* 2013). The ERA accumulated anomalies in Figure 4 are smaller in magnitude than MERRA cloud forcing anomalies, which are shown later.

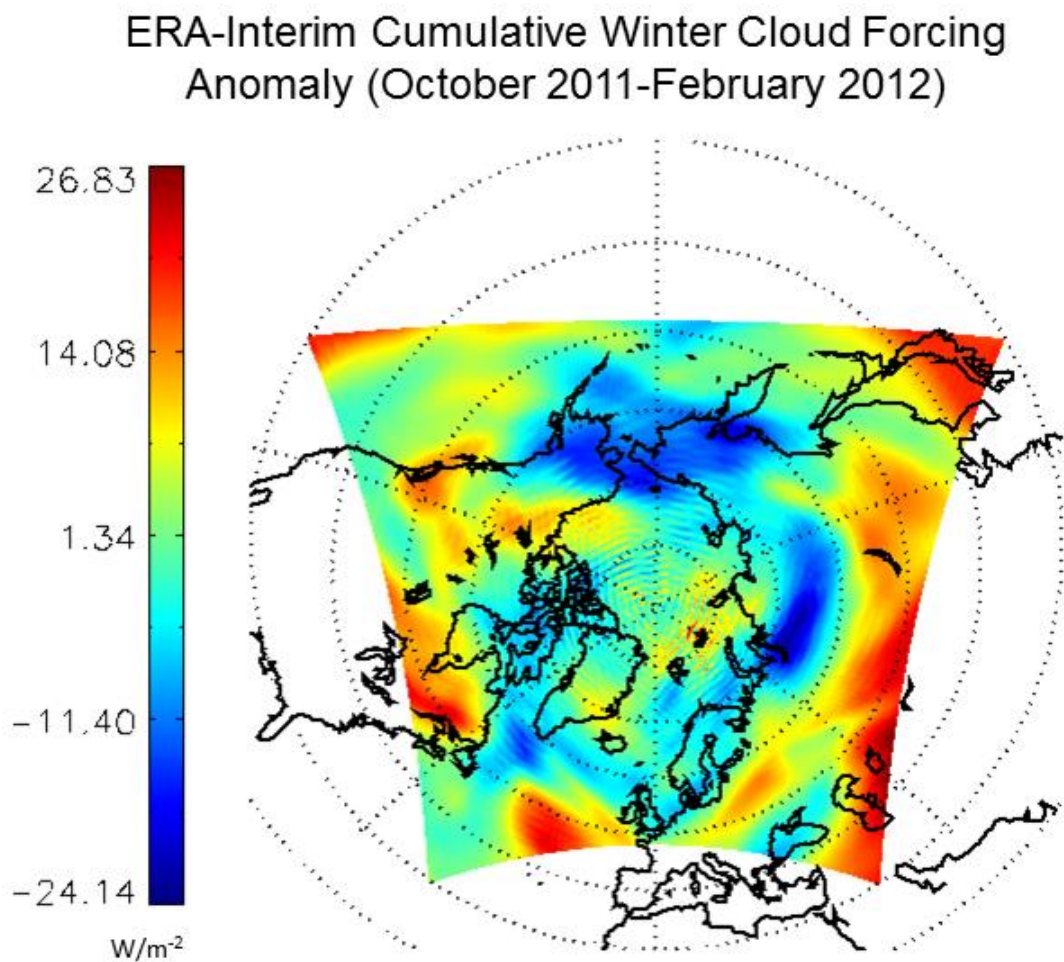


Figure 4. ERA-Interim surface cumulative longwave cloud forcing anomalies for October 2011- February 2012. Anomalies are calculated relative to the 2002-2012 mean for individual months.

From October 2011 to February 2012, Terra MODIS also showed positive cloud cover anomalies each month compared to the 2002-2012 mean spanning the Canadian Archipelago, Beaufort Sea, Chukchi Sea, and even into the Eastern Siberian Sea. MODIS cloud amount anomalies of +20% were observed north of the Alaskan and Siberian coastlines, yet the spatial pattern of anomalous cloud cover over the winter months varied. Similar spatial patterns of MODIS cloud amount and MERRA cloud forcing anomaly for November 2011 and January 2012 are provided for comparison (Figure 5). ERA-Interim cloud forcing anomalies and the MODIS cloud amount product disagreed with MERRA cloud forcing only in that they did not show a significant positive cloud anomaly off the east coast of Greenland. Though the cloud forcing anomalies in this region are very high, the ice dynamics off the northeast coast of Greenland readily transport ice southward into warmer, open water. Significant cloud forcing in this region, therefore, does not contribute significantly to the Arctic sea ice cover. The cloud cover anomaly in the Beaufort Sea during January was over one standard deviation above normal, and though other months' positive anomalies between October and February were not above one standard deviation, they contributed to a cloudy 2011-2012 winter season.

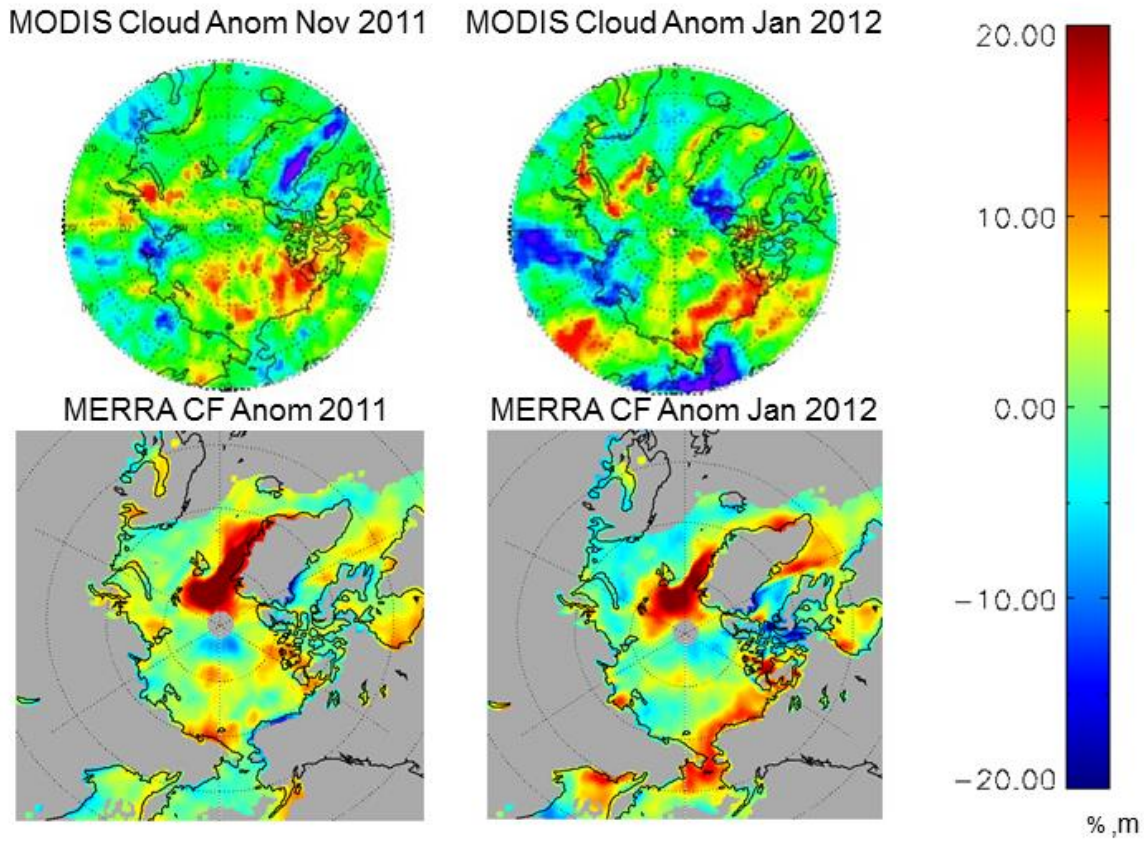


Figure 5. Cloud cover anomalies (%) in November 2011 and January 2012 (top left and right, respectively) from Terra MODIS, and cloud forcing anomaly (Wm^{-2}) in November 2011 and January 2012 from the MERRA reanalysis (bottom left and right, respectively). The anomalies are calculated relative to the monthly means for the periods of 2002-2012 for both Terra MODIS and MERRA.

Remote sensing can provide verification of increased Arctic cloud over the winter months, as satellites provide unmatched coverage of the Arctic at a fine spatial resolution. Detecting and understanding the Arctic's unique cloud feedbacks and properties presents many challenges to traditional passive solar- and thermal infrared-based remote sensing, however. A study by Liu et al. (2009) sought to evaluate the biases in MODIS cloud detection. By comparing cloud observations with CloudSat and CALIPSO, MODIS biases in cloud detection over open water and ice cover were determined. As sea ice concentration of a surface increases, MODIS

detects fewer clouds as compared to a combined CALIPSO-CloudSat "truth" product, meaning MODIS that has a negative bias in cloud detection over ice compared to other satellite products. The same study concluded that over open water, however, MODIS cloud mask performed with minimal error.

When using MODIS cloud cover products to support model reanalysis output, these biases must be addressed. In our analysis, the MODIS cloud cover product showed positive cloud cover anomalies over the Beaufort and Chukchi Seas from October 2011- February 2012. Throughout these months, there was little change in sea ice concentration over the regions of interest. Varying sea ice concentration would have produced biases on the month-to-month level since the MODIS cloud cover is sensitive to changes in ice concentration (Frey et al. 2008). For the November-February period, the areas showing positive anomalies were ice-covered. In this case, the MODIS cloud detection negative bias supports our claim of enhanced winter cloud cover in the 2011-2012 by possibly underreporting what was still a significant amount of positive cloud anomaly. In October, positive MODIS cloud cover anomalies were observed over open water in the Beaufort Sea. This measurement may be accepted with minimal bias, if any, due to improved performance of the MODIS cloud mask over scenes with open water. Though MODIS detects less cloud than active satellite lidar/radar sensors over ice, MODIS cloud mask still observed significant positive cloud cover anomalies throughout the winter of 2011-2012.

Using the Thorndike (1992) method previously discussed, sea ice growth resulting from the October 2011-February 2012 positive cloud radiative forcing anomaly is calculated based on cloud forcing from MERRA (Figure 5). Sea ice loss greater than 45 cm occurs over the Canadian through Siberian Arctic over the winter season. This area of anomalously positive winter cloud forcing corresponds to the September 2013 sea ice record minima in the Canadian Archipelago

and Beaufort Sea, as well as areas of extremely reduced sea ice in the Chukchi and Eastern Siberian Seas.

While the ice concentration anomalies in Figure 6 match the general location of the changes in thickness due to winter cloud forcing, their spatial patterns are far from identical. The northward and westward shift of the September ice concentration from the winter thickness anomalies can be partially explained by ice drift. The region of the Arctic in Figure 6 has its ice motion dominated by the Beaufort Gyre and the Transpolar Drift Stream (Serreze and Barry 2005), where the specific circulations of these features are explained later. Sea ice motion vectors in 2012 from the Polar Pathfinder daily, 25 km EASE-Grid product (Fowler *et al* 2013) were used to move the initial sea ice thickness anomaly field in Figure 6. After applying the ice motion field from the end of February 2012 to the beginning of September of the same year, the final, ‘drifted’ ice growth over the entire Arctic is shown in Figure 7. The thinned ice from October-February that resulted from increased downwelling cloud forcing, advected with sea ice

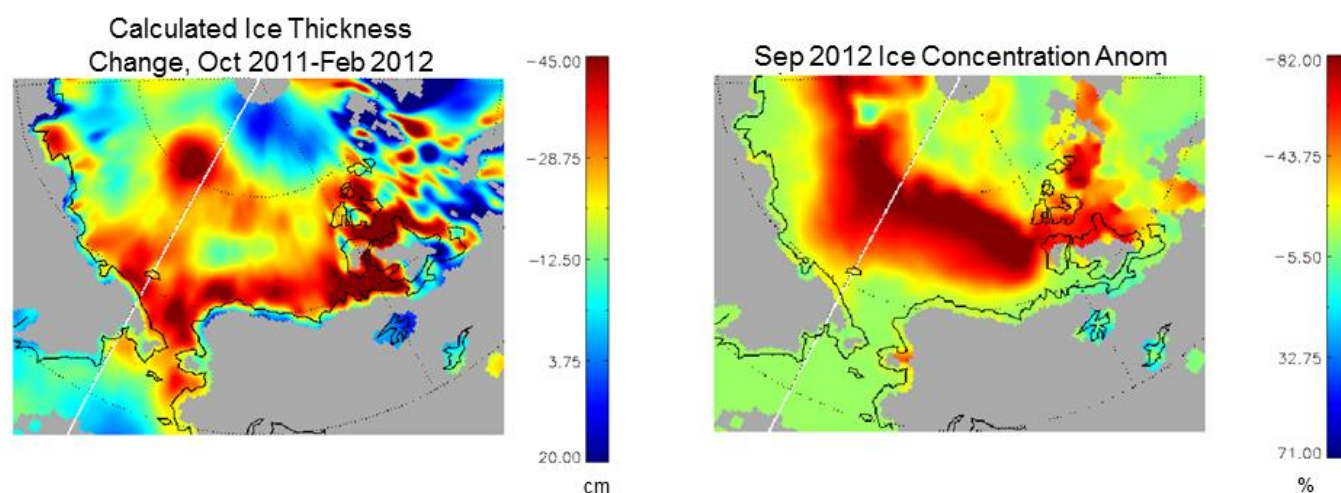


Figure 6. Change in ice thickness estimated from MERRA net cloud radiative forcing from October 2011-March 2012, where gray represents land areas and areas (left). Sea ice concentration anomalies for September 2012 from SSMIS observation relative to the 1982-2013 mean (right).

motion data, is significant across the Beaufort, Chukchi, and Eastern Siberian Seas. This corresponds well to the anomalously low sea ice concentration over those regions in September, shown in Figure 6. The drifted ice accumulation is also low in the northern Kara, Laptev, and Barents Sea, which also matches ice concentration anomalies in that region.

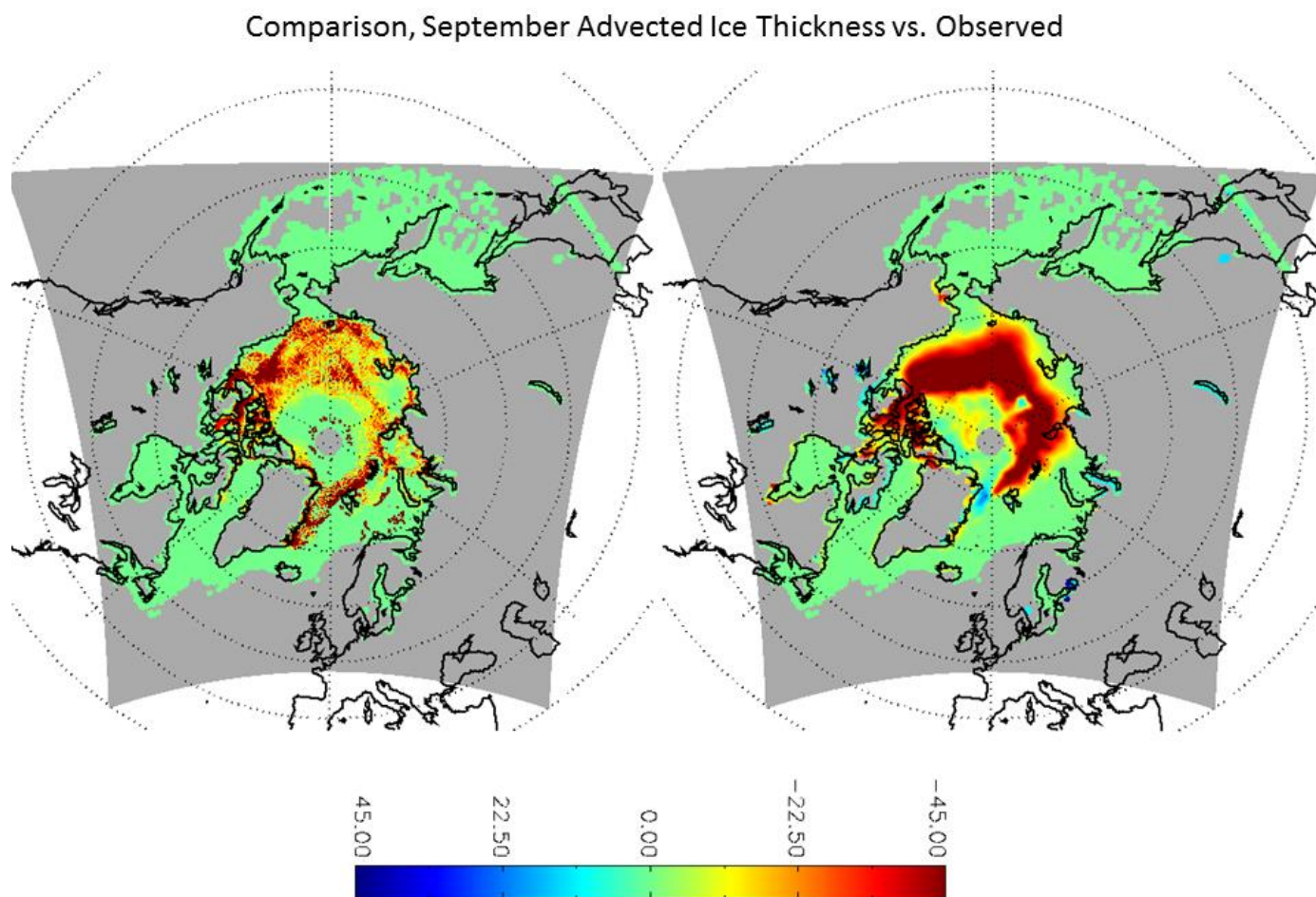


Figure 7. Ice thickness distribution anomalies (cm) at the beginning of September due to ice drift where green represents areas with sea ice drifted away or that did not have significant ice concentration anomalies (left). Sea ice concentration anomalies (%) for September 2012 from SSMIS observations relative to the 1982-2013 mean (right).

Decreased ice concentration in this region of the Arctic Ocean portends decreased ice concentration for much of the interior Arctic. Located north of the semi-permanent Aleutian

Low, this area is heavily trafficked by storm systems that can bring high winds. The thin, first-year ice shields the thicker ice of the Central Arctic from the deleterious effects of high winds and possible warm air advection brought northward by the storm track. Thinner or scant coverage of ice in this region will be more quickly eroded by insolation, warm air advection, and liquid precipitation that the summer brings, leaving the shrinking region of multi-year ice exposed.

4. Winter 1984 Cloud Amount

As discussed above, the winter of 2011-2012 exemplified ice changes under extensive, positive cloud forcing anomaly which decreased end-of-summer sea ice concentration. Over the satellite record, cloud anomaly have shown significant variability on both decadal and yearly scales. In opposition to 2012, when excess cloud cover aided in ice loss, the winter of 1983-1984 saw widespread decreased Arctic cloud cover that ultimately contributed to areal increase of 20% September sea ice over the Beaufort Sea than average, in addition to anomalously positive ice concentrations over the entire Arctic Basin (NSIDC). Liu and Key (2014) demonstrated that minimal winter cloud cover in 2013 increased September ice concentration and area, but to a greater extent than the 1983-1984 case.

Though far from producing a sea ice maximum, this negative seasonal cloud forcing anomaly could be considered typical for the first-half of the remote sensing record, when ice concentration anomalies in the Beaufort region were generally positive. This event predates current-generation satellite remote sensing products by nearly a decade, and as such, verification is limited. Agreement between the MERRA (Figure 8) and ERA (Figure 9) reanalyses output are in consensus over the region of interest, and are presented here for comparison. Both models show an area of greatly decreased cloud forcing centered over the Beaufort and Chukchi Seas. Less cloud cover in winter decreases the amount re-emitted longwave radiation upon the surface, resulting in cooler surface temperatures. These lower temperatures accelerate the formation of sea ice over areas of open water and promote increased thickness of existing ice.

Differences between the two models in regions besides the Beaufort are less subtle than in the 2011-2012 case. Namely, the ERA output shows positive cloud cover anomalies over the

Canadian Archipelago, while the same MERRA variable shows negative anomalies of a similar magnitude. Disregarding model differences elsewhere, both agree that fewer clouds in the winter months of 1983-1984 allowed for ample surface cooling and increased ice concentration through the summer. MERRA cumulative cloud forcing anomaly shows a dense region of negative values over the Beaufort Sea as low as -50 Wm^{-2} . ERA shows lower cloud

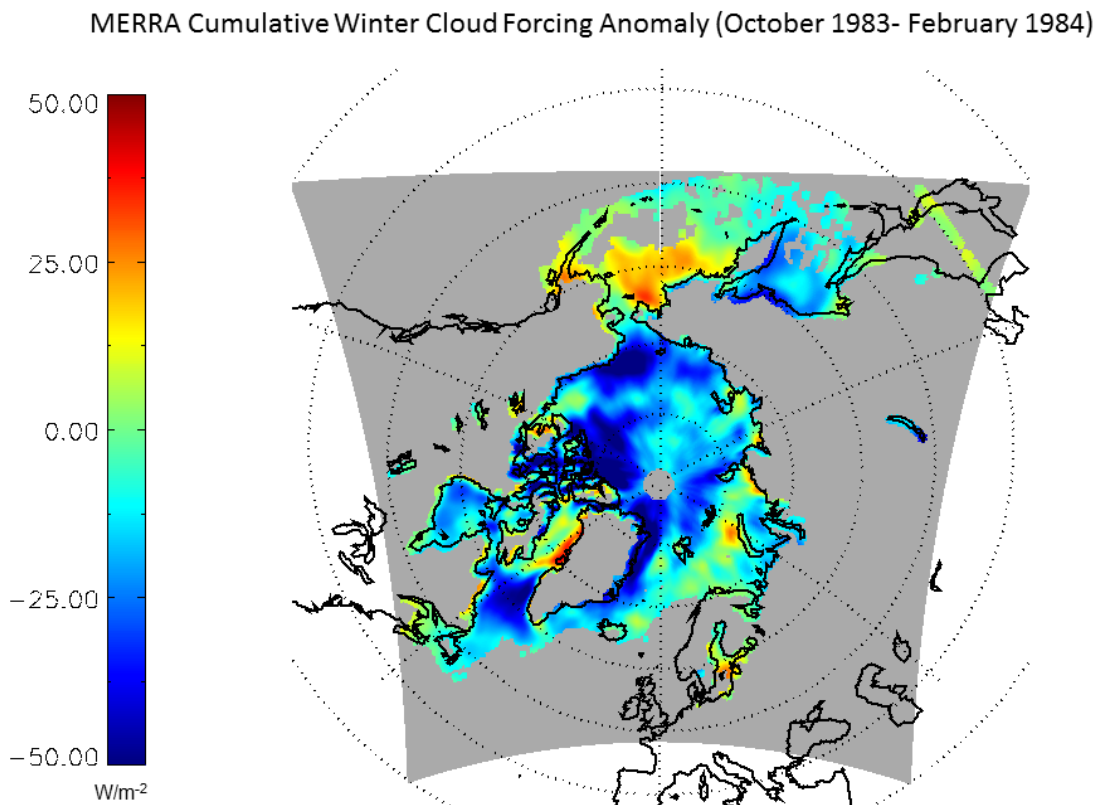


Figure 8. Cumulative cloud forcing anomaly (Wm^{-2}) from October 1983 to March 1984 from the MERRA reanalysis. The anomalies are calculated relative to the monthly means for the period 1982-2013.

forcing anomalies than MERRA (Figure 8), but still recorded regions of the Beaufort and Chukchi seas experiencing more than 35 Wm^{-2} of additional cooling.

ERA-Interim Cumulative Winter Cloud Forcing Anomaly (October 1983-February 1983)

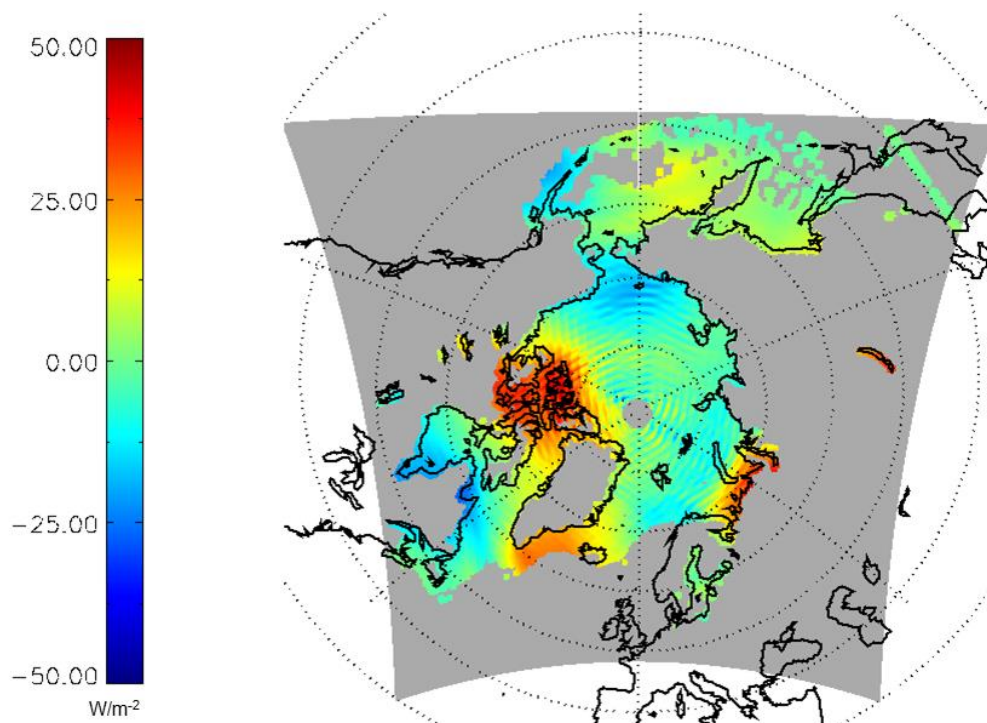


Figure 9. Cumulative cloud forcing anomaly (Wm^{-2}) from October 1983 to March 1984 from the ERA reanalysis. The anomalies are calculated relative to the monthly means for the period 1982-2013.

The Thorndike (1992) model may again be used to determine the effects of the 1983-84 winter on the Beaufort and Chukchi sea ice (Figure 10). MERRA cloud forcing anomaly showed negative anomalies that motivated greater than 45 cm of ice growth at the surface along the northern coastlines of Alaska and Siberia. Ice concentration anomalies were positive near the Canadian Archipelago, which agrees with ERA-Interim reanalysis rather than MERRA.

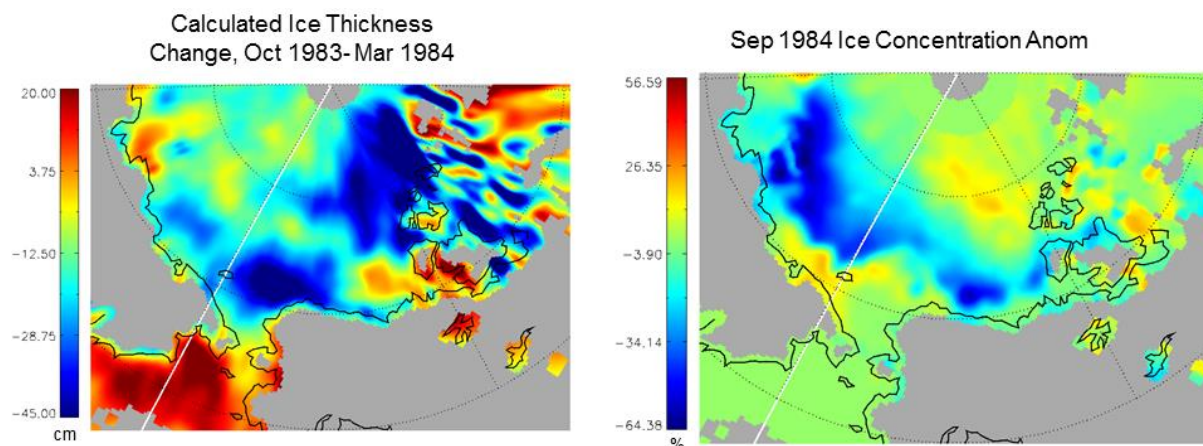


Figure 10. Change in ice thickness estimated from MERRA net cloud radiative forcing from October 1983-March 1984, where gray represents land areas and areas (left). Sea ice concentration anomalies for September 1984 from SSMIS observation relative to the 1982-2013 mean (right).

The redistribution from February to September of these anomalies due to ice drift would likely resemble the observed ice concentration anomalies in September 1984. Generally, the Beaufort Gyre circulates ice from the Alaskan and Siberian coastline in a clockwise pattern away from the Canadian Archipelago. The westward advection of thickness anomalies may have increased ice concentrations similar to what is shown in observed concentration anomalies. The increase in concentration in this marginal Arctic ice region has far-reaching implications for ice area extent in late summer. The increase in sea ice concentration in this marginal Arctic region has far-reaching implications for ice area extent in late summer. This shelf of first-year ice between 70°-80° north serves as a buffer to the core of Central Arctic multi-year ice, absorbing the brunt of sensible heat fluxes from northward-tracking storm systems as well as warmer waters from the Bering Sea.

5. Climatological Relationship between Cloud Forcing and Sea Ice Concentration, 1982-2013

While cloud forcing can provide a significant radiative contribution to low and high ice years, the evolution of cloud forcing anomalies over the last three decades implies that they play a role in determining Arctic sea ice concentrations in a broader, climatological sense. How frequently have significant wintertime cloud anomalies influenced summertime sea ice anomalies over the last three decades?

The satellite record has provided a remotely-sensed sea ice climatology that may be compared with cloud radiative forcing. Climate reanalysis cloud forcing anomalies are tabulated with ice concentration as early as 1982 and through 2013, giving a record that dates back 32 years. Regions of interest are limited to marginal sea ice zones, as the contribution of cloud forcing over thin sea ice can most dramatically effect ice growth and loss. The cloud forcing anomaly is calculated relative to the 1982-2013 mean. In many cases, monthly cloud forcing anomalies can exceed $\pm 20 \text{ Wm}^{-2}$, which represents a significant radiative forcing on the surface energy budget. Since cloud forcing anomaly has great variance in both magnitude and spatial distribution, the anomaly summation method described in the methods section was used to achieve the most realistic approximation of cloud behavior over a winter season.

The connection between wintertime cloud forcing anomaly and summertime sea ice concentration anomalies calculated from MERRA and passive microwave data may be determined by performing the pixel-by-pixel correlation between both variables over from 1982-2013. This 32-year timeframe for the reanalysis was chosen to match the period covered by APP-x, from which ice thicknesses were obtained. Figure 11 shows strong inverse relationships over

much of the Canadian Archipelago, Beaufort, and Chukchi Seas. Small regions of the Central Arctic exhibit direct relationships between cloud forcing anomaly and sea ice concentration anomaly, but the thick multi-year ice present there causes it to be outside the scope of this study. The thin seasonal ice cover in the Beaufort Sea is very sensitive to changes in the surface energy budget. As a result, anomalies in cloud forcing during the winter can drastically alter the sea ice concentration of the region. The significant inverse correlation between anomalous cloud forcing and the ice concentration anomaly over the Beaufort Sea implies that variations in cloud cover may appreciably alter the surface energy budget, though this is a statistical relationship that does not prove causality. Furthermore, this connection suggests that trends in ice concentration over this region may be explained by trends in surface warming or cooling caused by changing cloud cover.

Correlation: MERRA 6-month CF Anomaly with September Ice Conc. Anomaly

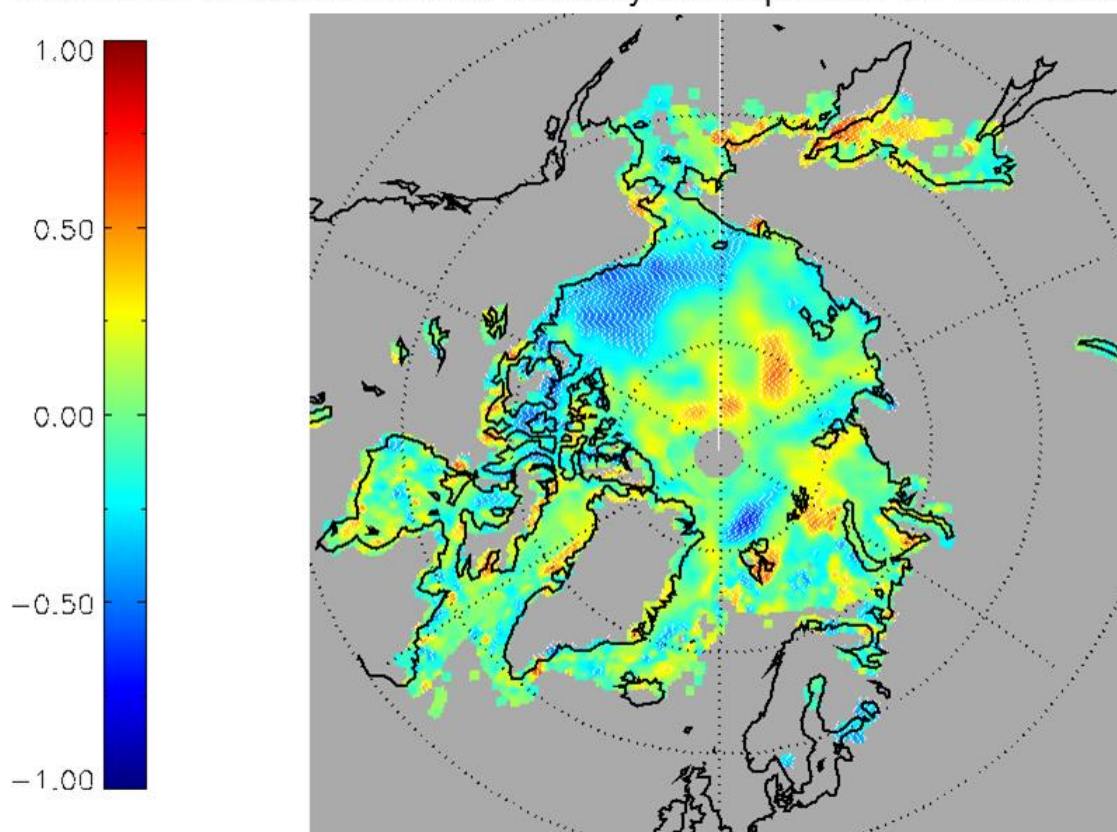


Figure 11. Point-by-Point mapping of correlations between MERRA cumulative October-March net cloud radiative forcing anomaly and SSMIS September sea ice concentration anomaly the following summer from 1982-2013. Stippling indicates statistical significance at the .95 confidence level.

In order to demonstrate that the results are not an artifact of a single climate reanalysis, ERA-Interim cloud forcing anomalies were also used to analyze the relationship between wintertime cloud cover and summer ice concentration. Both reanalyses showed similar areas of positive cloud cover anomaly during winter over the 2011-2012 case study, so similar correlation results were expected. The two models generally agreed on the relationship between clouds and sea ice in the region of study, yet showed some spatial differences (Figure 12). ERA and MERRA agreed that cumulative winter cloud forcing anomalies were strongly inverse to September ice concentrations over the Chukchi Sea, Eastern Siberian Sea, and Canadian

Archipelago. Cloud cover over the Beaufort Sea, however, had a much lower statistical coherence and significance in the ERA-Interim correlation map. Globally, ERA-based cloud forcing also shows strong inverse relationships with ice concentration in the Baffin and Newfoundland Bay as well as the Sea of Okhotsk.

The clouds over these regions do not all have similar methods of formation or internal properties. The Beaufort Sea, in particular, has been observed to contain high amounts of supercooled water clouds, rather than ice clouds (Hobbs and Rangno 1998). The supercooled liquid water significantly enhances longwave emission to the surface compared to ice, which may further strengthen the correlation in this region. Alternatively, an area with increased ice-phase clouds may experience less emission to the surface per cloud amount, resulting in a weaker correlation. This difference in cloud phase may aid in explaining the reduced coherence in some regions of the Arctic.

Correlation: ERA 6-month CF Anomaly with September Ice Conc. Anomaly

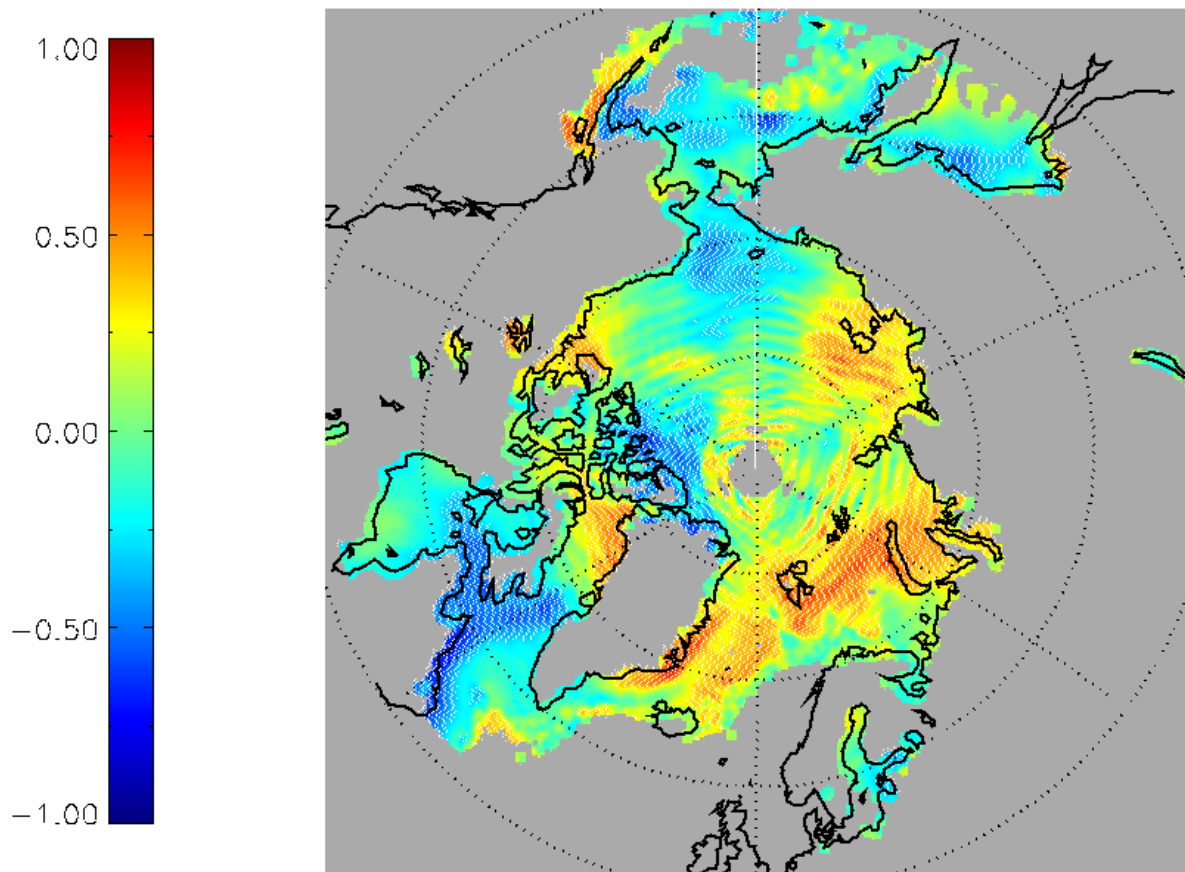


Figure 12. Point-by-Point mapping of correlations between ERA cumulative October-March net cloud radiative forcing anomaly and SSMIS September sea ice concentration anomaly the following summer from 1982-2013. Stippling indicates statistical significance at the .95 confidence level.

Much like the MERRA correlation map, direct relationships between cloud forcing and ice concentration are observed in regions of the Arctic where sea ice concentrations are dynamically, rather than radiatively, controlled (Figures 11 and 12). The Transpolar Drift Stream pushes sea ice southward through the Fram Strait, resulting in a zone of high ice divergence rather than a marginal ice zone. Similarly, the warm water from the Gulf Stream moderates surface energy budgets from the Greenland Sea to the Barents Sea such that sensible heat flux

poses a stronger control on sea ice than longwave flux. In some cases, ice concentration may even force cloud cover (Figure 13).

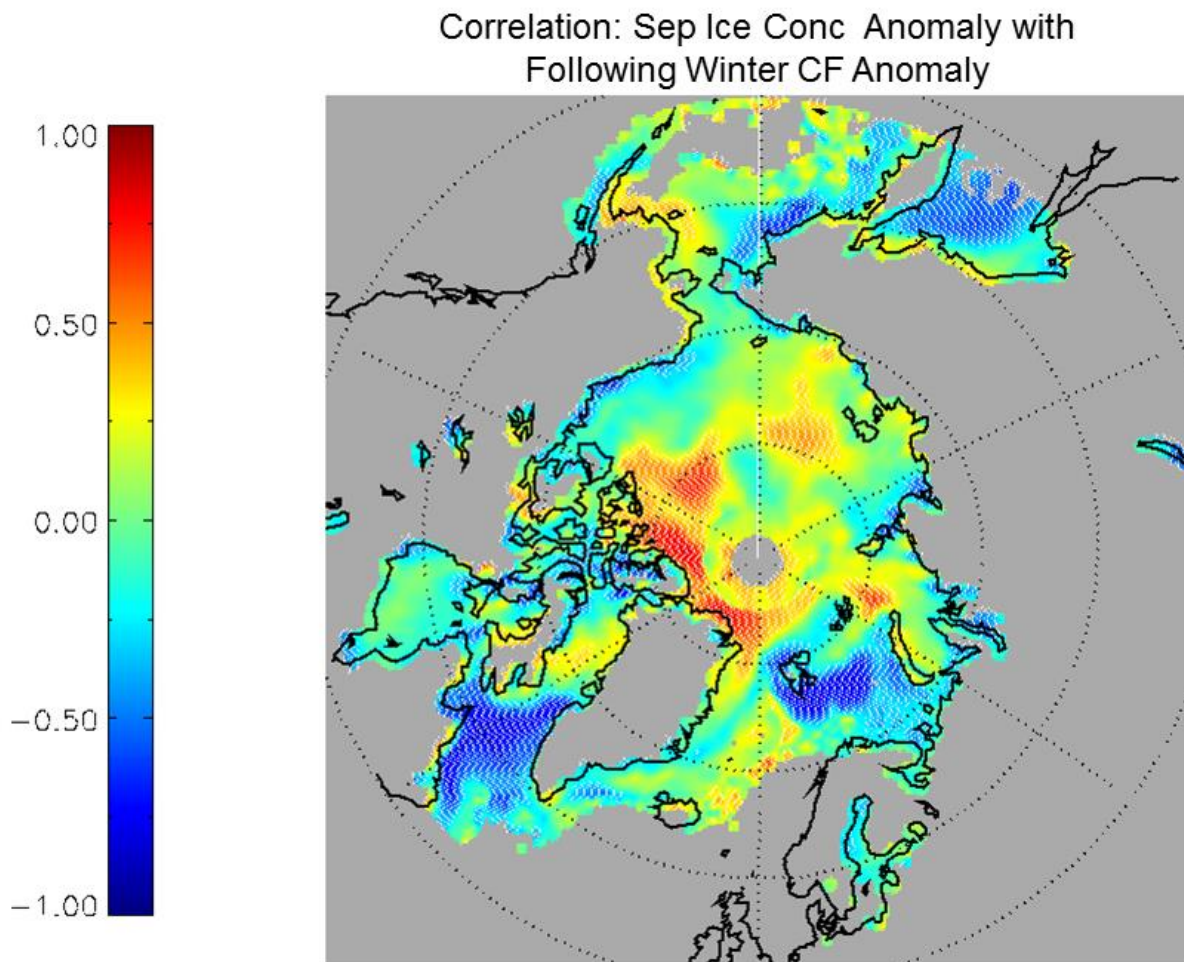


Figure 13. Point-by-Point mapping of correlations between SSMIS September sea ice concentration anomaly and MERRA cumulative October-March net cloud radiative forcing anomaly the following winter from 1982-2013. Stippling indicates statistical significance at the .95 confidence level.

Though it is well-documented that changes in sea ice concentration cause changes in cloud cover and other cloud properties (Vavrus et al 2009, 2011, Schweiger et al 2008a, Cuzzone and Vavrus 2011, Kay and Gettelman 2009, Palm et al 2010, Liu et al 2012a), the ability for clouds to alter sea ice concentrations is more significant in the Beaufort Sea and surrounding

regions. Even a thin layer of sea ice can decouple the ocean from the lower atmosphere and have an appreciable effect on liquid water path in the atmosphere (Barton and Veron 2012). By this logic, September ice concentration anomaly in over the Beaufort Sea had an inverse correlation with the cloud forcing anomaly for the following winter, but the relationship was neither as statistically significant nor strong as cloud anomalies forcing sea ice changes in the Beaufort Sea (Figure 13).

Other Arctic regions such as the Fram Strait and Barents Sea show large magnitudes of high and low correlation, respectively. While the sea ice in these regions is partially moderated by typical thermal and radiative processes, ice dynamics and modes of atmospheric circulation play strong roles in the ice concentration of these areas. The north shoreline of Greenland and the Canadian Archipelago is the site of ice convergence, where multi-year ice queues to be ejected southward from the Fram Strait, and should not be considered a marginal ice zone. The eastern portion of the Barents sea represents a terminus of the Gulf Stream, where year-round transport of warm water significantly affects ice concentrations.

Though the relationship between the ice concentration of a region in September and its cloud forcing (derived from cloud cover) the following winter bears comment, it is not the focus of this work. Ice concentration in September has a weak inverse correlation with cloud forcing the following winter. This result is expected, as the presence of sea ice in September serves to impede cloud formation at small spatial and timescales, as discussed in Barton and Veron (2012). As a region becomes ice-covered over winter, September ice wanes as a predictor of cloud behavior in this study's region of interest. This weakening of September ice concentration's influence on a locale's cloud cover is demonstrated in Figure 14. The magnitude of correlation between the variables over the Beaufort Sea region peaks in October, when the two signals are

compared less than 30 days apart. As the time between these signals increases, both the magnitude and statistical significance decrease over the Beaufort. By December, the strength of the correlation is approaching zero, indicating that while ice may determine cloud behavior in early winter, they do not appreciably affect cloud forcing throughout the ice freezing season. Very high correlations west of the Canadian Archipelago imply that the sea ice there forces cloud cover up to three months into the future. The cause of this statistical relationship is unknown.

Correlation: Sep. Ice Conc. Anom. with Months in Following Winter

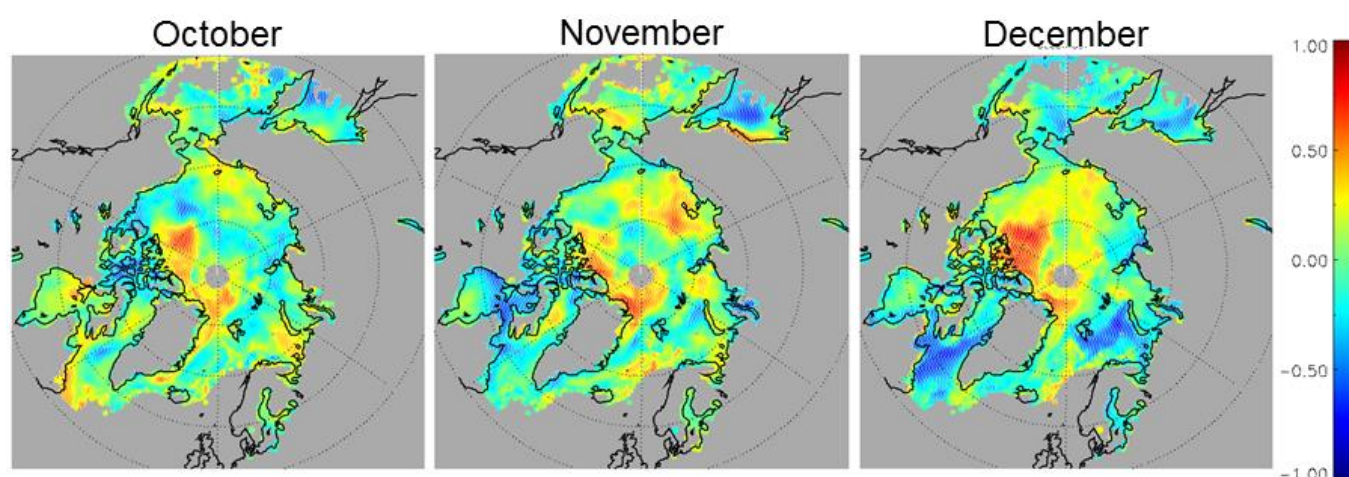


Figure 14. Point-by-Point mapping of correlations between and SSMIS September sea ice concentration anomaly and MERRA cloud radiative forcing anomaly during October, November, and December of the following winter from 1982-2013. Stippling indicates statistical significance at the .95 confidence level.

Passive microwave observations provide a record of ice concentration anomaly in the Beaufort Sea. Figure 15 compares the six-month accumulated cloud forcing anomalies with ice concentration anomalies in a bar plot time series. The data suggest a strong, inverse relationship between cloud forcing and ice concentration anomaly that is maintained throughout the satellite

record, where low (high) ice summers occur after winters with high (low) cloud forcing anomalies. The bar plot shows a period of increased sea ice concentration in the Beaufort Sea from 1982-1996 followed by a period of decreased ice concentration from 1997-2013, resulting in a general trend of decreasing sea ice concentration from 1982-2013.

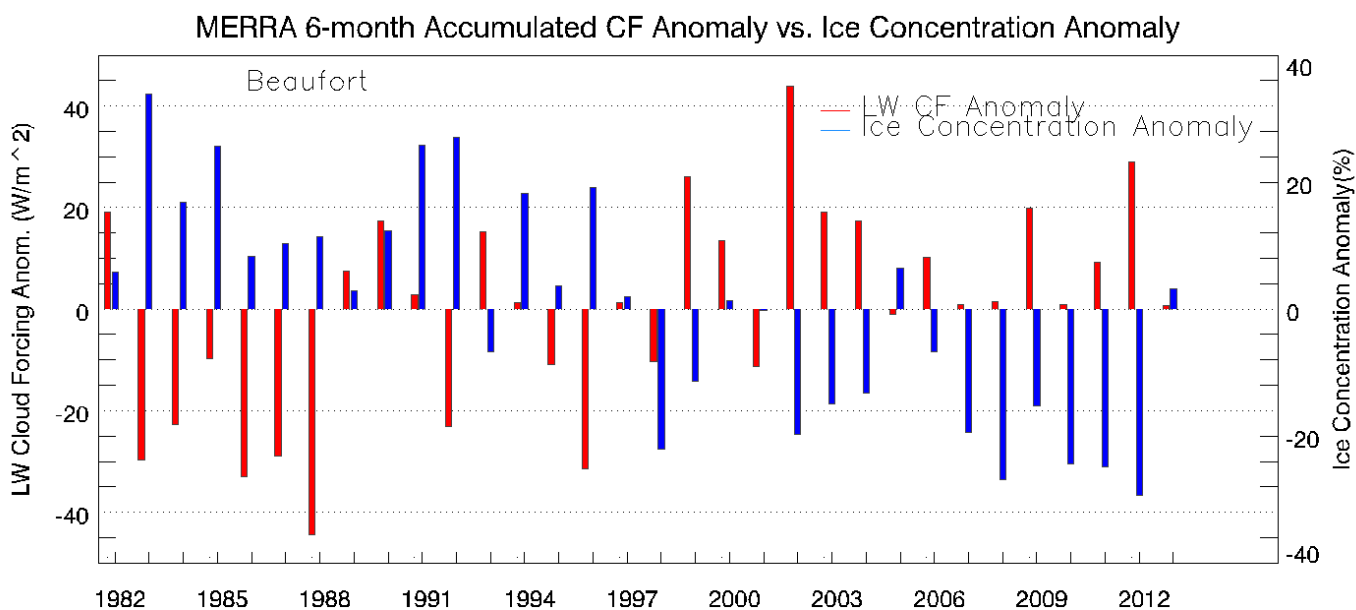


Figure 15. Time series comparing cumulative October-March cloud forcing anomalies (red) with September ice concentration anomaly (blue) over the Beaufort Sea region. Anomalies are calculated relative to the 1982-2013 mean.

The time series may be separated into two distinct, fifteen-year regimes of cloud forcing. Consistent, negative cloud forcing from 1982-1996 represents a lack of cloud cover over the Beaufort Sea from October through March each year. Fewer clouds increased the surface's ability to cool directly to space and spurred sea ice growth over this period. The Beaufort Sea experienced an increase in ice concentration and thickness during this relative absence of clouds. In the next fifteen years, greatly increased cloud forcing was observed concurrently with unprecedented low sea ice concentrations.

6. Influences of Wintertime Cloud forcing on Summertime Sea Ice Concentration

The two regimes of cloud forcing in Figure 14 represent the two modes of influence that cloud forcing anomaly has on sea ice. In the Beaufort Sea, the contribution of cloud forcing changes its behavior around 1997. Before this inflection point cloud forcing anomaly acted to increase ice thickness by approximately 0.15 m per year, after the inflection point cloud forcing anomalies decreased ice thickness by a similar yearly amount. From 1982-1997, the summed contribution of anomalous cloud forcing allowed 170 W m^{-2} to escape from the surface. Using the earlier described method, this corresponds to a potential increase in sea ice thickness of 1.45 m. From 1997-2012 the cumulative effect of cloud forcing supplied an excess of 170 W m^{-2} , allowing for a potential ice thickness decrease that overwrites contributions from the previous regime of anomalously negative cloud forcing.

Differences in ice concentration over this time period can be analyzed by comparing yearly ice concentration anomalies at the beginning and end of the decadal regime (Figure 15). An area of negative sea ice concentration anomaly near the Canadian Arctic in 1982 was replaced by an area of positive ice concentration anomaly by 1996, and the Beaufort region experienced a marked increase in ice concentration over these years. Ice thickness increased by 0.15 m, similar to the global trend of increasing sea ice thickness in this time period. This increase is reflected in APP-x September sea ice thickness where a shelf of thin ($<0.5 \text{ m}$) ice can be seen extending towards the Alaskan-Canadian shoreline and through the Canadian Archipelago in 1996 that was not present in 1982.

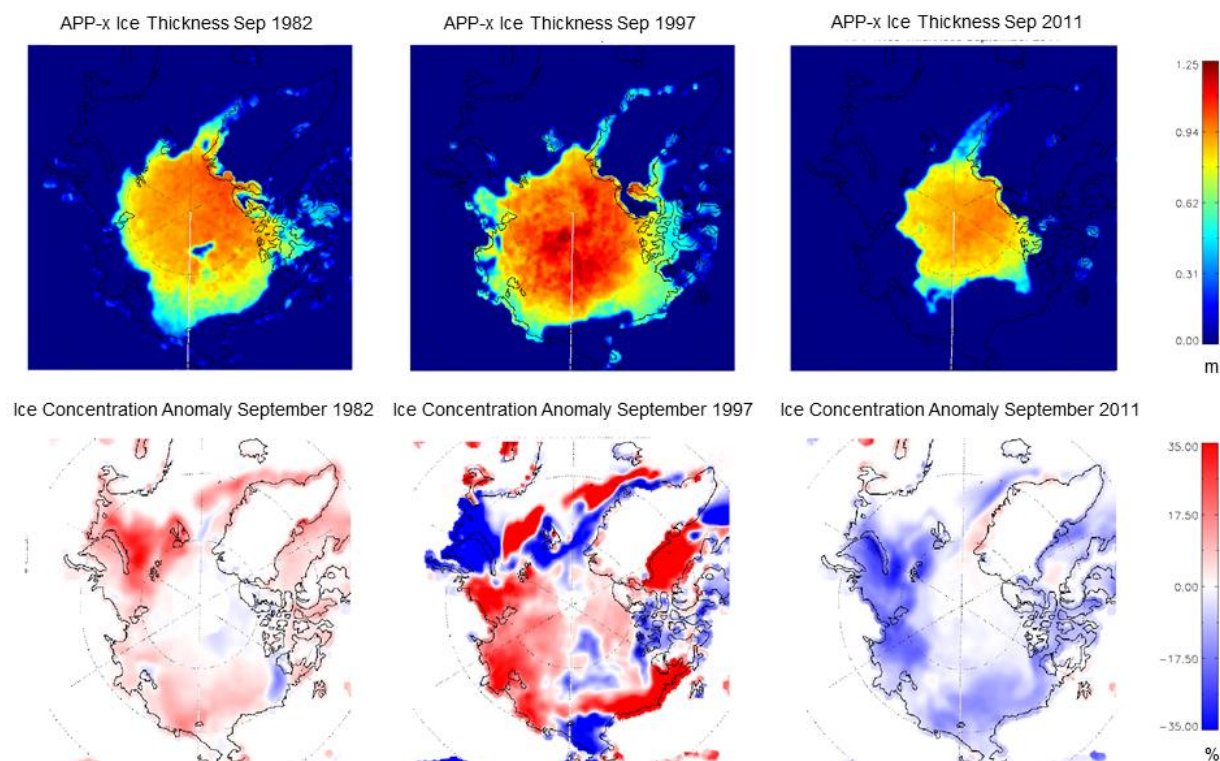


Figure 16. Ice thickness estimated from APP-x ice thicknesses in September of 1982, 1997, and 2011 (top left, middle, and right, respectively), where dark blue represents areas of land or negligible ice thickness. Sea ice concentration anomalies relative to the 1982-2013 mean in September of 1982, 1997, and 2011 (bottom left, middle, and right, respectively), where white represents areas of land or negligible sea ice concentration anomaly.

The second notable period of cloud forcing anomaly occurs from 1997-2011, and opposes 1982-1996 in that cloud forcing in that the second period was consistently anomalously positive and corresponds to a sea ice concentration decrease. Increased cloud cover over each year inhibited winter refreezing by trapping surface cooling and limiting ice formation. By 2011, an area of positive ice concentration anomaly along the western Canadian Archipelago in 1996 was replaced entirely with strong negative ice concentration anomalies over the entire region. The cloud forcing over these years had a striking effect on ice thickness in the Beaufort region. Thin (<0.5 m) ice present in the Beaufort Sea and Canadian Archipelago in 1996 had

disappeared almost entirely by 2002, leaving only the thick multi-year ice of the Central Arctic. Average thickness in the region decreased by .42 m, more than 6.5 times the global the decrease over the entire Arctic for the same period.

Clouds represent only one of many intricate processes governing changes in sea ice concentration. Surface temperature, synoptic weather patterns, and ocean dynamics can considerably alter ice concentrations. Still, winter cloud accounts for a significant portion of variance in the ice concentration. The portion of this variance explained by changes in cloud forcing may be further analyzed by performing a simple linear regression. Performed in Figure 16, the regression coefficient between cloud forcing and ice concentration anomaly is near -0.59, indicating changes in September Sea ice concentration may be attributed to cloud forcing over the winter months. This result is expected, considering that the surface heating and cooling contributions of cloud pale in comparison to effects of other climate feedbacks in the Arctic such as albedo and surface temperature (Pithan and Mauritsen 2013). Winter cloud forcing anomalies clouds do account, however, for over 35% of the variance in Beaufort Sea ice concentration. This lagged dependence of summer ice concentration on winter cloud demonstrates that the memory of marginal sea ice regions can be anywhere from 6-11 months.

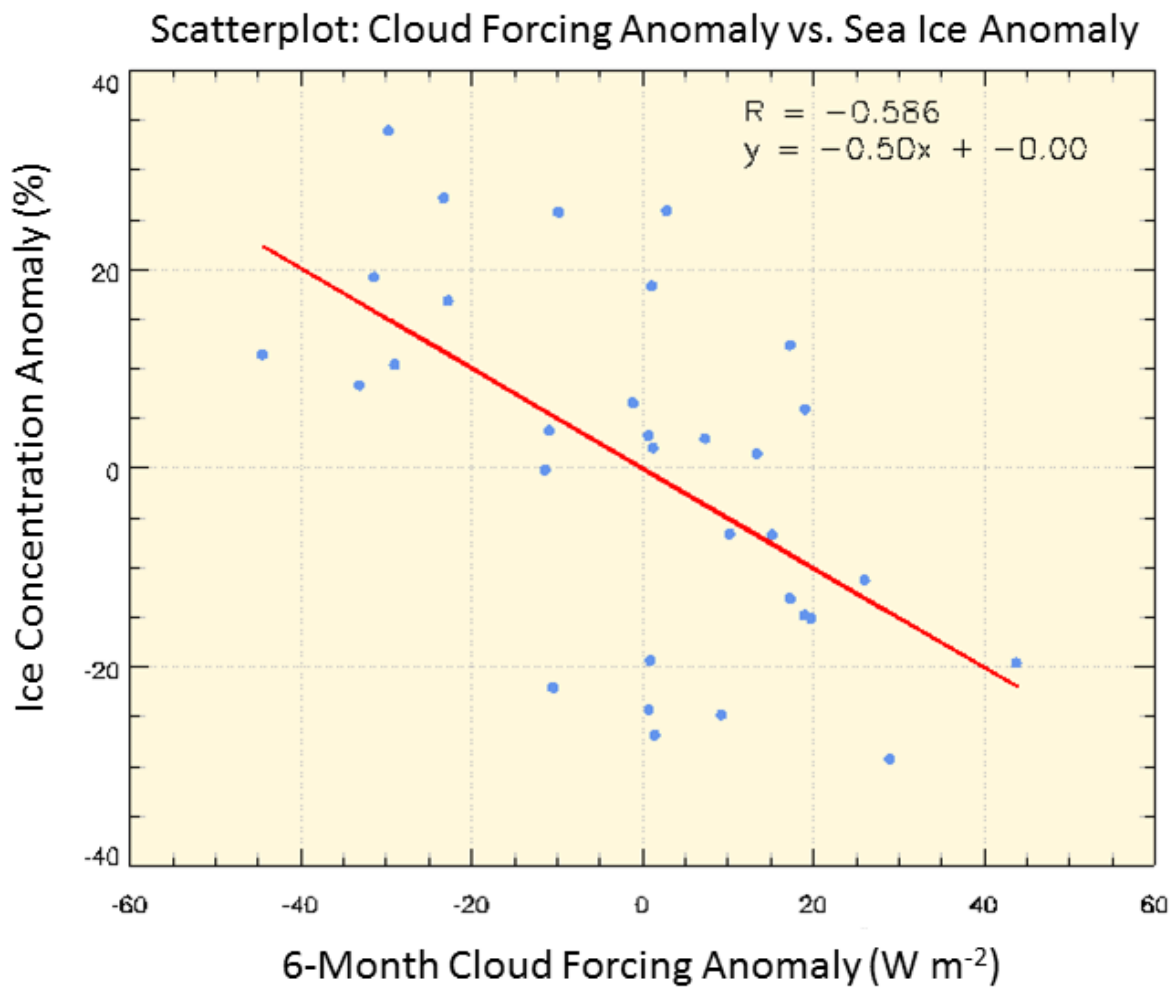


Figure 17. Linear regression of 6-month (October-March) cloud forcing anomaly ($W m^{-2}$) onto ice concentration anomaly in the Beaufort Sea Region. September ice concentration anomaly is represented by the vertical axis. The points (blue circles) from 1982-2013 are best fit here with a line of slope $y = -0.5x$.

The two opposing regimes of ice concentration and cloud forcing anomaly over the Beaufort Sea are possibly influenced by major atmospheric indices. Ballinger and Rogers (2014) examined the teleconnections between major atmospheric and oceanic indices and their effects on ice extent in the Beaufort and Chukchi Seas. Their findings indicate that seasonal changes in these indices could only explain significant sea ice loss after 1997, which corresponds to the regime of negative ice concentration anomalies and increased cloud forcing. They found that the El Niño-Southern Oscillation (ENSO) has influenced ice extent retreat in recent years via the strongly positive Pacific/North American Pattern (PNA), which typically brings above-average geopotential height anomalies as well as warmer temperatures over Alaska and Northwestern Canada. The analysis done in this study agrees with their results, finding no significant correlation between cloud forcing anomaly and ENSO indices nor sea ice concentration and ENSO indices when compared over the entire 1982-2013 time series (Figure 17). Similarly, correlations between ice concentration and cloud forcing with the Arctic Oscillation (AO) index were very weak ($< |0.10|$). The Pacific Decadal Oscillation (PDO), however, had correlations with ice concentrations and cloud forcing that were significant ($\approx |0.50|$). This result is to be expected, as negative PDO phases which have dominated since the late 1990s bring above-average surface temperatures to the Beaufort Region. None of the correlations between climate indices and ice concentration or cloud forcing had magnitudes surpassing the correlation of cloud forcing and ice concentration.

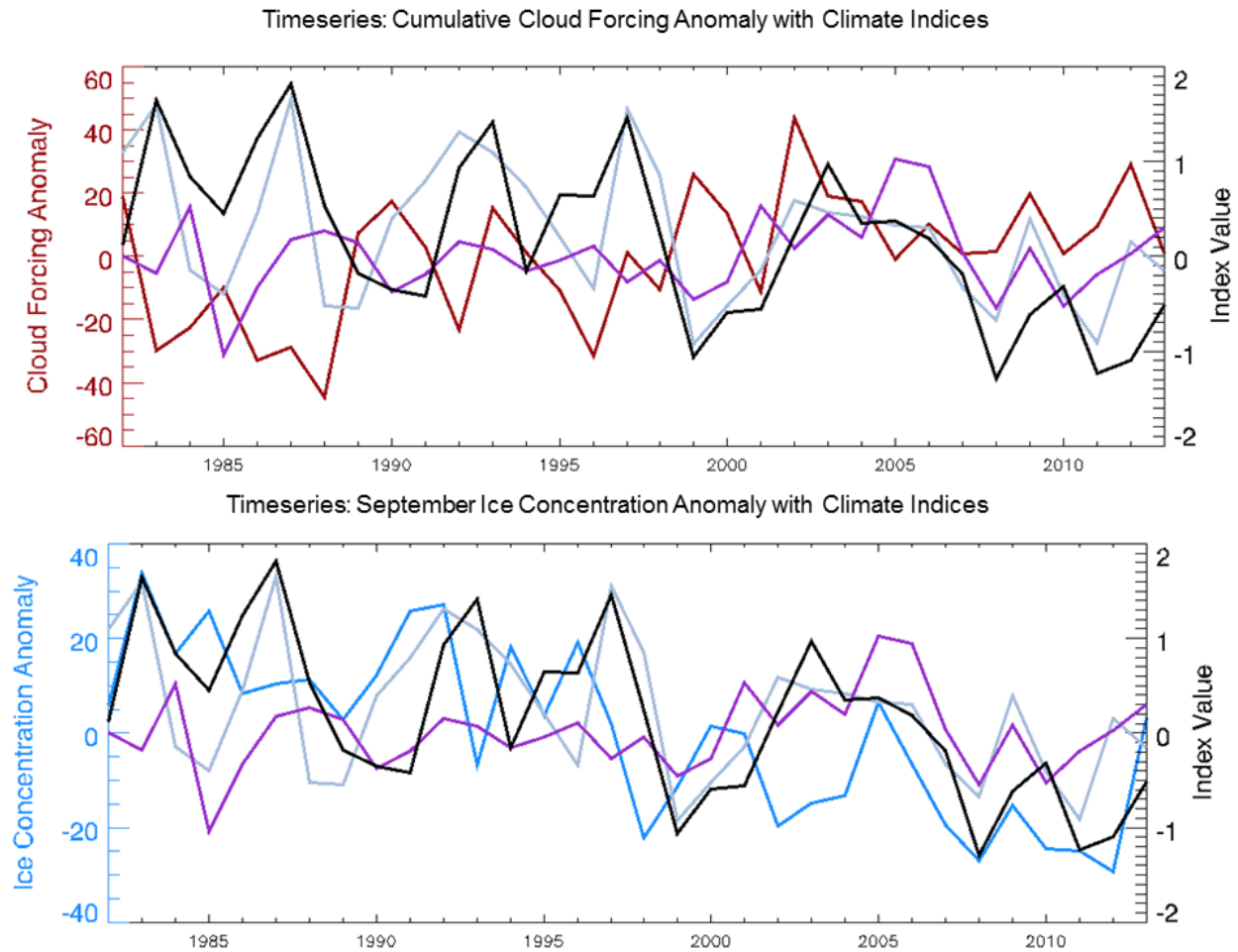


Figure 18. Time series of various climate indices with cloud forcing anomalies and ice concentration anomalies over the Beaufort Sea region. The first Figure shows cloud forcing anomaly (red) with ENSO, AO, and PDO indices (gray, purple, and black, respectively). The second column shows ice concentration (blue) anomaly with ENSO, AO, and PDO indices (gray, purple, and black, respectively)

Though the Beaufort Sea makes up only a portion of the Arctic Ocean, its location relative to large-scale atmospheric circulations allows changes in its ice concentration to impact Arctic sea ice on a much larger scale. The Beaufort Gyre is a wind-driven, anticyclonic circulation that advects ice westward from the Beaufort Sea across the Chukchi Sea and then northward from the Eastern Siberian Sea. While the strength of this circulation can vary, Liu *et al* (2014) showed that the Beaufort Gyre caused significant sea ice "drift" that redistributed first-

year ice from January to September of 2013. Over the satellite record, winter cloud forcing anomalies in the Beaufort Sea area show an extensive region of inverse correlation with September ice concentration anomalies throughout the Beaufort Gyre region (Figure 18). Large-scale atmospheric dynamics support this relationship. Over the winter months, ice altered by cloud forcing in the Beaufort Sea is then propelled by westward surface currents through the Chukchi and East Siberian Seas. Other processes, such as ocean heating, freshwater flux, and solar insolation may affect this correlation. Nevertheless, this statistical link between Beaufort Sea cloud cover and ice concentration across the Alaskan-Siberian Arctic adds significance to the anomalies in the Beaufort region.

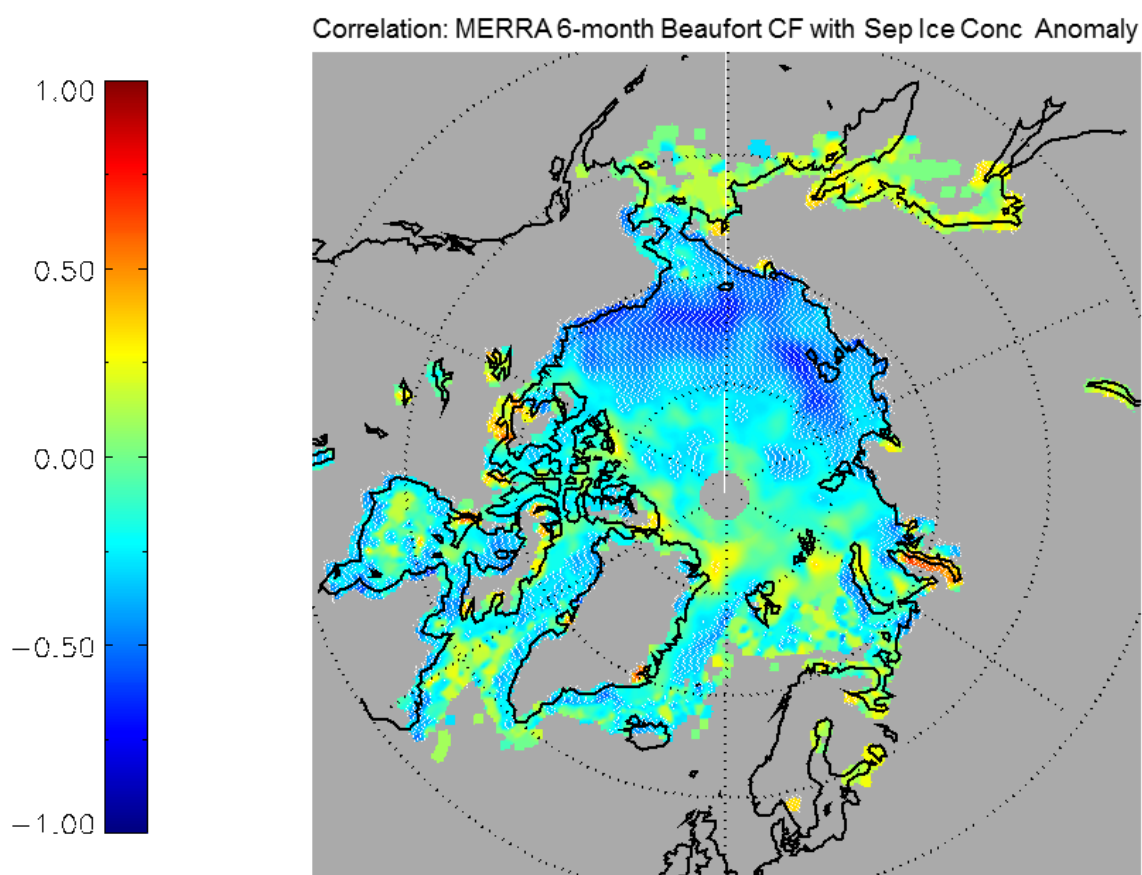


Figure 19. Point-by-Point mapping of correlations between MERRA cumulative October-March net cloud radiative forcing anomaly in the Beaufort Sea region and SSMIS September sea ice concentration anomaly the following summer from 1982-2013. Stippling indicates statistical significance at the .95 confidence level.

7. Conclusions

Recent observations of declining Arctic sea ice extent encompass numerous climate processes including clouds' radiative effects as well as atmospheric and oceanic heat transport. This study explores relationships between large-scale atmospheric and ocean circulations, surface air temperature, and ice dynamics to decreasing sea ice concentrations during the summer months. The implications of these processes on summer sea ice concentration are well-studied and can be found elsewhere (Serreze *et al* 2007, Francis *et al* 2012, Stroeve *et al* 2012). However, a consensus on the interplay between clouds, cloud changes to solar insolation, and sea ice extent anomalies has not been reached (cf, Nussbaumer and Pinker 2012, Kapsch *et al* 2013, Graverson *et al* 2011, Kay *et al* 2008, Schweiger *et al* 2008b, Kauker *et al* 2009). The analysis presented in this study demonstrates that winter cloud cover anomalies can have significant effects on summertime sea ice cover at inter-annual and decadal time scales.

September 2012 marked a record sea ice minimum for summertime ice extent over the satellite record. Marginal ice zones such as the Beaufort and Chukchi Seas during this time were almost entirely ice-free by the end of summer. Multiple satellite products agreed qualitatively with climate model reanalysis output showing that winter months preceding the 2012 minimum experienced cloud cover consistently above average in these regions from October 2011 through February 2012. More cloud in the Arctic winter results in a less negative surface radiation budget, decreasing cooling at the surface and hampering further ice growth. The cloud radiative effect was verified by satellite estimates and by climate model reanalysis output. Ice thickness

decrease in much of Beaufort Sea from the wintertime radiative anomaly was determined, theoretically, to be greater than 45 cm. Regions of calculated ice growth resulting directly from the positive cloud forcing anomalies in October-February were advected based on daily ice motion fields from March through August. The drifted sea ice growth anomaly pattern shows striking similarities to ice concentration anomalies with ice concentration anomalies in September not only over the Beaufort and Chukchi Seas, but the entire Arctic. Accordingly, positive cloud cover anomalies in the 2011-12 winter were a key contributor to the September 2012 sea ice minimum. Though not examined thoroughly in this study, anomalies in downwelling shortwave over the summer months could have contributed to this extensive ice loss. Preliminary analysis of cloud cover anomalies from MODIS Aqua and Terra do not show extraordinary decreases in cloud cover (which would increase downwelling shortwave radiation striking the surface), and even some positive cloud anomalies over the region of interest in July and August.

An examination of wintertime cloud forcing anomaly from 1982-2013 over the Beaufort Sea region showed two separate regimes of both September sea ice concentration and October-March cloud forcing anomaly which varied inversely with one another. From 1982-1997, cloud cover was generally lower than average, resulting in a more strongly negative surface radiation budget and further encouraging ice growth during the winter. As expected, this period had consistently higher September ice concentration anomalies. The accumulated monthly contribution of negative cloud forcing anomaly was used to make a rough approximation of ice thickness change, and showed that enhanced radiative cooling could provide 1.45 meters of ice thickness growth over the sixteen-year period. This value of decreased ice thickness, however, could range substantially based on the behavior of other affective variables during this time

period. Over the next sixteen years, 1998-2013, cloud cover over the Beaufort Sea and surrounding area was above average, while sea ice concentration anomaly was typically negative. The resulting anomalous cloud forcing contributed, cumulatively, enough downwelling longwave energy to decrease ice thickness by nearly 1.45 meters. Ice thickness changes were calculated from the method presented by Thorndike (1992). Areas of estimated ice thickness growth and loss that resulted directly from the winter cloud forcing anomalies corresponded spatially to satellite-derived thicknesses.

A corridor of the Arctic spanning from the central Canadian Archipelago as far east as the north shore of the Kamchatka peninsula was the domain of the case studies as well as the cloud and ice climatologies. The benefits for analyzing seasonal ice patterns are two-fold, as this region preliminarily showed an extensive range in ice concentration and seasonal cloud cover and has also been frequently referenced in current scientific literature (Kaye et al. 2007, Liu and Key 2014). Ice area anomalies over the Beaufort Sea trace a pattern similar to the ice anomaly of the entire Northern Hemisphere, implying that ice changes here act as a gauge for the rest of the Arctic. Thinner ice in the Beaufort Sea can be more easily broken up by Pacific cyclones, which frequently track through this region. By analyzing the preconditioning of this ice by winter cloud, the susceptibility of this regions to storm-caused summer breakup may be determined months in advance. Research suggests that ice coverage in this region also contributes to the phase of large-scale circulations that, in turn, force ice extent and dynamics in other parts of the Arctic (Rodionov *et al* 2007).

Changes in large-scale circulations affect cloud cover and thereby cause significant changes to the surface energy budget. This study found that circulation patterns such as the Beaufort Gyre increase the significance of local cloud anomalies in an Arctic-wide context.

Large-scale circulation, as represented in various climate indices also affects ice thickness and concentration changes in the winter. Though the ENSO and AO indices showed little relationship with clouds or ice concentration, the PDO average yearly index showed significant correlation with sea ice concentration anomalies in the Beaufort-Chukchi Seas area. No correlation between climate indices and ice concentration or cloud forcing anomaly had coherence greater than the relationship between wintertime cloud cover and September ice concentration.

In general, the strength of relationship between large-scale atmospheric indices and anomalies in both clouds and ice were notable, but did not have higher magnitudes of correlation than between corresponding years of cloud cover and sea ice concentration anomalies. This implies that while modes of atmospheric circulations may affect the Arctic system on a broad scale, there are regions of the Arctic that are more influenced by local contributors to the surface energy budget. The Beaufort Sea, Chukchi Sea, and Canadian Archipelago are proven statistically to be among these regions.

Here, it is demonstrated that cloud cover greater than one standard deviation above the mean over the Beaufort Sea region in the winter of 2012 led to an excess of downwelling longwave radiation to the surface energy budget, and that this anomaly in surface radiation contributed to the record minimum sea ice area in September of the same year. Encouraged by the effects of winter cloud forcing anomaly on summer sea ice extent, cloud trends were examined on a climatological basis. Over the course of the 32-year satellite record, cloud forcing over winter periods was shown capable of imposing a significant radiative forcing on marginal sea ice areas. This contribution can enhance or diminish trends of decreasing Arctic ice area, even in the face of increasing global temperatures.

8. Future Work

While this analysis was limited to two in-depth case studies, the climatology (Figure 14) of ice concentration and cloud forcing anomaly suggests that other years may have had significant ice melting events caused by cloud forcing anomalies. Future work will assess the exact contributions of winter clouds on these years of outlying ice concentration. For years of anomalous ice extent, it would be prudent to evaluate the spring and summer months (April-August) to determine whether downwelling shortwave radiation was also greatly modified by clouds, and had a synergistic effect with winter cloud cover anomaly. Though the results presented here are chiefly related to the Beaufort Sea, cloud forcing is a critical agent of change in many other marginal ice areas.

Multi-year trends in cloud cover undoubtedly exist in regions of the Arctic besides the Beaufort, and though the correlation maps presented here imply significant relation elsewhere, the cause of this linkage is not explored in-depth. Additionally, correlations between winter cloud forcing-derived changes in ice thickness will be performed only after these anomalies have been advected through September. This technique changes the variables of comparison, where advected thickness anomalies caused by cloud will be compared to ice concentration, instead of cloud forcing over ice concentration in the same pixel. Other regions of the Arctic such as the Laptev and Kara Seas warrant detailed studies of their own, as preliminary analysis observed that they may experience dramatic year-to-year variability of both cloud and sea ice concentration.

Regarding years of vastly anomalous sea ice concentration, the contributions of other variables must be assessed in contribution to these extreme events. It is very likely that the host of complex radiative and dynamical processes that govern the Arctic surface energy budget will

often supersede the energetic contribution exerted by changes in cloud cover. The strong linear trend in this ice concentration shows a lack of year-to-year variability that implies a monotonic increase to the surface energy budget over the satellite record. Understanding the inter-annual variability and forcing by Arctic clouds will also require the consideration of additional variables. Synoptic variability, bringing both strong cyclonic and anticyclonic circulations to the marginal regions of the Arctic can heavily alter cloud cover on short time frames, may be one source of the year-to-year variance of winter cloud forcing anomaly, and bears further investigation.

This study was focused solely on winter cloud cover and its effects on the surface radiation budget of marginal ice zones. Cloud cover after April and before October was not taken into consideration. Clouds have a surface cooling effect from June-August (Schweiger and Key 1994), and significant anomalies during these months will further add on to or offset the winter preconditioning of sea ice. The downwelling solar flux incident on the Arctic surface during summer months is large enough that cloud anomalies at intra-monthly timescales during the summer may also have large effects on sea ice concentration. Finer temporal resolution is needed to further investigate these processes. While winter clouds have shown to impose noticeable changes to summer ice extent, year-long monitoring and assessment of polar cloud cover will become crucial in determining both the near and distant future of the changing Arctic.

Acknowledgements

This work was supported by the NOAA National Climatic Data Center (NCDC) and the Joint Polar Satellite System (JPSS) Program Office. We are grateful to the University of Illinois Cryosphere Today website (<http://arctic.atmos.uiuc.edu/cryosphere/>) for providing their preliminary ice thickness estimates to the scientific community for evaluation. We thank R. Stone and C. Cox for valuable discussions on this work. We also thank M. Tschudi for providing the 2013 Polar Pathfinder daily 25 km EASE-Grid sea ice motion data. The MODIS data used in this study were acquired as part of the NASA's Earth-Sun System Division and archived and distributed by the MODIS Adaptive Processing System (MODAPS).

References

- Ackerman S.A., R.E. Holz, R. Frey, E.W. Eloranta, B.C. Maddux and M. McGill, 2008, Cloud detection with MODIS. Part II: validation, *J. Atmos. Ocean. Technol.*, **25**, 1073–86.
- Ackerman S.A., K.I. Strabala, W.P. Menzel, R.A. Frey, C.C. Moeller, and L.E. Gumley, 1998, Discriminating clear sky from clouds with MODIS, *J. Geophys. Res.-Atmos.*, **103**, 32141–57.
- Ballinger T.J. and J.C. Rogers, 2014, Climatic and atmospheric teleconnection indices and western Arctic sea ice variability, *Physical Geograpy*, **35**, 459-477.
- Barton N.P. and D.E. Veron, 2012, Response of clouds and surface energy fluxes to changes in sea-ice cover over the Laptev Sea (Arctic Ocean), *Climate Res.*, **54**, 69–84, doi:10.3354/cr01101.
- Cavalieri D.J., C.L. Parkinson, P. Gloersen, and H. Zwally, 1996, Sea Ice Concentrations from Nimbus-7 SMMR and DMSP SSM/I-SSMIS Passive Microwave Data (Boulder, CO: NASA DAAC at the National Snow and Ice Data Center [2002–2013]). (updated yearly)
- Curry J.A., W.B. Rossow, D. Randall, and J.L. Schramm. 1996, Overview of Arctic cloud and radiation characteristics, *J. Clim.*, **9**,1731–64.
- Cuzzone J. and S. Vavrus, 2011, The relationships between Arctic sea ice and cloud-related variables in the ERA-Interim reanalysis and CCSM3, *Environ. Res. Lett.*, **6**, 014016.
- Dee D.P. *et al.*, 2011, The ERA-Interim reanalysis: configuration and performance of the data assimilation system, *Q. J. R. Meteorol. Soc.*, **137**, 553–97.
- Deser C. and H. Teng, 2008, Evolution of Arctic sea ice concentration trends and the role of atmospheric circulation forcing, 1979–2007, *Geophys. Res. Lett.*, **35**, L02504.
- Eisenman I., N. Untersteiner, and J.S. Wettlaufer, 2007, On the reliability of simulated Arctic sea ice in global climate models, *Geophys. Res. Lett.*, **34**, L10501.
- Fowler C., W. Emery, and M. Tschudi, 2013, *Polar Pathfinder Daily 25 km EASE-Grid Sea Ice Motion Vectors. Version 2* (Boulder, CO: National Snow and Ice Data Center).
- Francis J.A., W. Chan, D.J. Leathers, J.R. Miller and D.E. Veron, 2009, Winter northern hemisphere weather patterns remember summer Arctic sea ice extent, *Geophys. Res. Lett.*, **36**, L07503.

- Frey R.A., S.A. Ackerman, Y. Liu, K.I. Strabala, H. Zhang, J.R. Key, and X. Wang, 2008, Cloud detection with MODIS. Part I: improvements in the MODIS cloud mask for collection 5, *J. Atmos. Ocean. Technol.*, **25**, 1057–72.
- Graversen R, T. Mauritsen, S. Drijfhout, M. Tjernström, and S. Mårtensson, 2011, Warm winds from the Pacific caused extensive Arctic sea-ice melt in summer, 2007, *Clim. Dyn.*, **36**, 2103–12.
- Hobbs P. and A. Rangno, 2006, Microstructures of low and middle-level clouds over the Beaufort Sea, *Q.J.R. Meteorol. Soc.*, **124**, pp. 2035-2071.
- Holland M.M. and C.M. Bitz, 2003, Polar amplification of climate change in coupled models *Clim. Dyn.*, **21**, 221–32.
- Holz R.E., S.A. Ackerman, F.W. Nagle, R. Frey, S. Dutcher, R.E. Kuehn, M.A. Vaughan, and B. Baum, 2008, Global Moderate Resolution Imaging Spectroradiometer (MODIS) cloud detection and height evaluation using CALIOP, *J. Geophys. Res.*, **113**, D00A19.
- Intrieri J.M., C.W. Fairall, M.D. Shupe, P.O.G. Persson, E.L. Andreas, P.S. Guest, and R.E. Moritz, 2002, An annual cycle of Arctic surface cloud forcing at SHEBA, *J. Geophys. Res.*, **107**, 8039.
- Kapsch M.L., R.G. Graversen, and M. Tjernström, 2013, Springtime atmospheric energy transport and the control of Arctic summer sea-ice extent, *Nature Clim. Change* **3** 744–8.
- Kauker F., T. Kaminski, M. Karcher, R. Giering, R. Gerdes, and M. Voßbeck, 2009, Adjoint analysis of the 2007 all time Arctic sea-ice minimum, *Geophys. Res. Lett.*, **36**, L03707.
- Kay J.E. and A. Gettelman, 2009, Cloud influence on and response to seasonal Arctic sea ice loss, *J. Geophys. Res.-Atmos.*, **114**, D18204.
- Kay J.E., T. L'Ecuyer, A. Gettelman, G. Stephens, and C. O'Dell, 2008, The contribution of cloud and radiation anomalies to the 2007 Arctic sea ice extent minimum, *Geophys. Res. Lett.*, **35**, L08503.
- Key J., D. Slayback, C. Xu, and A. Schwieger, 1999, New climatologies of polar clouds and radiation based on the ISCCP D products, *Proc. 5th Conf. on Polar Meteorology and Oceanography* (Boston, MA: Am. Meteorol. Soc.), 227–32.
- Liu Y., S.A. Ackerman, B.C. Maddux, J.R. Key, and R.A. Frey, 2010, Errors in cloud detection over the Arctic using a satellite imager and implications for observing feedback mechanisms, *J. Clim.*, **23**, 1894–907.
- Liu Y., J.R. Key, Z. Liu, X. Wang, and S.J. Vavrus, 2012a, A cloudier Arctic expected with diminishing sea ice, *Geophys. Res. Lett.*, **39**, L05705.

- Liu Y., J. Key, J. Francis, and X. Wang, 2007, Possible causes of decreasing cloud cover in the Arctic winter 1982–2000, *Geophys. Res. Lett.*, **34**, L14705.
- Liu Y., J.R. Key, R. Frey, S. Ackerman, and W.P. Menzel, 2004, Nighttime polar cloud detection with MODIS, *Remote Sens. Environ.*, **92**, 181–94.
- Liu Y., J.R. Key, and X. Wang, 2008, The influence of changes in cloud cover on recent surface temperature trends in the Arctic, *J. Clim.*, **21**, 705–15.
- Liu Y., J.R. Key, and X. Wang, 2009, Influence of changes in sea ice concentration and cloud cover on recent Arctic surface temperature trends, *Geophys. Res. Lett.*, **36**, L20710.
- Liu Y. and J.R. Key, 2014, Less winter cloud aids summer 2013 Arctic sea ice return from 2012 minimum, *Environ. Res. Lett.*, **9**, 044002.
- Maslanik J. and J. Stroeve, 1999, *Near-Real-Time DMSP SSM/I-SSMIS Daily Polar Gridded Sea Ice Concentrations* (Boulder, CO: NASA DAAC at the National Snow and Ice Data Center) [2002–2013]. (updated daily)
- Nussbaumer E.A. and R. T. Pinker, 2012, The role of shortwave radiation in the 2007 Arctic sea ice anomaly, *Geophys. Res. Lett.*, **39**, L15808.
- Ogi M. and I.G. Rigor, 2013, Trends in Arctic sea ice and the role of atmospheric circulation, *Atmos. Sci. Lett.*, **14**, 97–101.
- Overland J.E., J.A. Francis, E. Hanna and M. Wang, 2012, The recent shift in early summer Arctic atmospheric circulation, *Geophys. Res. Lett.*, **39**, L19804.
- Overland J.E. and M. Wang, 2013, When will the summer Arctic be nearly sea ice free?, *Geophys. Res. Lett.*, **40**, 2097–101.
- Palm S.P., S.T. Strey, J. Spinhirne, and T. Markus, 2010, Influence of Arctic sea ice extent on polar cloud fraction and vertical structure and implications for regional climate, *J. Geophys. Res.-Atmos.*, **115**, D21209.
- Perovich D K, Richter-Menge J A, Jones K F and Light B 2008 Sunlight, water, and ice: extreme Arctic sea ice melt during the summer of 2007 *Geophys. Res. Lett.* **35** L11501
- Pithan F. and T. Mauritsen, 2013, Arctic amplification dominated by temperature feedbacks in contemporary climate models, *Nature Geosci.*, **7**, 181–84.
- Rienecker M.M. *et al.*, 2011, MERRA: NASA’s modern-era retrospective analysis for research and applications, *J. Clim.*, **24**, 3624–48.
- Rodionov S.N. , N.A. Bond, and J.E. Overland, 2007, The Aleutian Low, storm tracks, and winter climate variability in the Bering Sea, *Deep-Sea Res.*, **54**, 2560–77.

- Sato K., J. Inoue, and M. Watanabe, 2014, Influence of the Gulf Stream on the Barents Sea ice retreat and Eurasian coldness during early winter, *Environ. Res. Lett.*, **9**, 084009.
- Schweiger A.J., 2004, Changes in seasonal cloud cover over the Arctic seas from satellite and surface observations, *Geophys. Res. Lett.*, **31**, L12207.
- Schweiger A. and J.R. Key, 1994, Arctic Ocean radiative fluxes and cloud forcing estimates from the ISCCP C2 cloud dataset, *J. Appl. Meteorol.*, **33**, 948–63.
- Schweiger A.J., R.W. Lindsay, S. Vavrus, and J.A. Francis, 2008a, Relationships between Arctic sea ice and clouds during autumn, *J. Clim.*, **21**, 4799–810.
- Schweiger A.J., J. Zhang, R.W. Lindsay, and M. Steele, 2008b, Did unusually sunny skies help drive the record sea ice minimum of 2007?, *Geophys. Res. Lett.*, **35**, L10503.
- Serreze M. C. and R. G. Barry, 2005, The Arctic climate system, Cambridge: University Press, Chapter 7.
- Serreze M.C. and J.A. Francis, 2006, The arctic amplification debate, *Clim. Change*, **76**, 241–64.
- Serreze M.C., M.M. Holland, and J. Stroeve, 2007, Perspectives on the Arctic's shrinking sea-ice cover, *Science*, **315**, 1533–6.
- Stone R.S., 1997, Variations in western Arctic temperature in response to cloud radiative and synoptic-scale influences, *J. Geophys. Res.*, **102**, 21769–76.
- Stone R.S., D. Douglas, G. Belchansky, and S. Drobot, 2005, Correlated declines in Pacific Arctic snow and sea ice cover, *Arctic Res. United States*, **19**, 18–25.
- Stroeve J.C., M.C. Serrez, M.M. Holland, J.E. Kay, J. Maslanik, and A.P. Barrett, 2012, The Arctic's rapidly shrinking sea ice cover: a research synthesis, *Clim. Change*, **110**, 1005–27.
- Thorndike A.S., 1992, A toy model linking atmospheric thermal radiation and sea ice growth, *J. Geophys. Res.*, **97**, 9401–10.
- Tjernström M., J. Sedlar, and M.D. Shupe, 2008, How well do regional climate models reproduce radiation and clouds in the Arctic? An evaluation of ARCMIP simulations, *J. Appl. Meteorol. Climatol.*, **47**, 2405–22.
- Vavrus S., M.M. Holland, and D.A. Bailey, 2011, Changes in Arctic clouds during intervals of rapid sea ice loss, *Clim. Dyn.*, **36**, 1475–89.
- Vavrus S., D. Waliser, A. Schweiger, and J. Francis, 2009 Simulations of 20th and 21st century Arctic cloud amount in the global climate models assessed in the IPCC AR4, *Clim. Dyn.*, **33**, 1099–115.

- Wang X.J. and J.R. Key, 2003, Recent trends in arctic surface, cloud, and radiation properties from space, *Science*, **299**, 1725–8.
- Wang X.J. and J.R. Key, 2005, Arctic surface, cloud, and radiation properties based on the AVHRR Polar Pathfinder dataset. Part II: recent trends, *J. Clim.*, **18** 2575–93.
- Wang J., J. Zhang , E. Watanabe, M. Ikeda, K. Mizobata, J.E. Walsh, X. Bai, and B. Wu, 2009, Is the Dipole Anomaly a major driver to record lows in Arctic summer sea ice extent?, *Geophys. Res. Lett.*, **36**, L05706.
- Wang X., J. Key, and Y. Liu, 2015, Algorithm Theoretical Basis Document for the Extended AVHRR Polar Pathfinder (APP-x) Dataset, National Oceanic and Atmospheric Administration, 82 pp.
- Zhang X. and J.E. Walsh, 2006, Toward a seasonally ice-covered Arctic Ocean: scenarios from the IPCC AR4 model simulations. *J. Clim.*, **19**, 1730–47.